ISTANBUL TECHNICAL UNIVERSITY ★ GRADUATE SCHOOL OF SCIENCE ENGINEERING AND TECHNOLOGY

DESIGN OF NEW TYPE HIGH EFFICIENCY MAGNETIC GEAR

M.Sc. THESIS

Sadra Mousavi

Department of Electrical and Electronics Engineering
Electrical Engineering Program

MAY 2015

ISTANBUL TECHNICAL UNIVERSITY ★ GRADUATE SCHOOL OF SCIENCE ENGINEERING AND TECHNOLOGY

DESIGN OF NEW TYPE HIGH EFFICIENCY MAGNETIC GEAR

M.Sc. THESIS

Sadra Mousavi
504111063

Department of Electrical and Electronics Engineering
Electrical Engineering Program

Thesis Advisor: Asst. Prof. Dr. Fuat Küçük

MAY 2015

İSTANBUL TEKNİK ÜNİVERSİTESİ ★ FEN BİLİMLERİ ENSTİTÜSÜ

YÜKSEK VERİMLİ MANYETİK DİŞLİ KUTUSU TASARIMI

YÜKSEK LİSANS TEZİ

Sadra Mousavi
504111063

Elektronik ve Elektrik Mühendisliği
Elektrik Mühendisliği Programı

Tez Danışmanı: Yrd. Doç. Dr. Fuat Küçük

MAYIS 2015

Sadra Mousavi, a **M.Sc.** student of ITU **GRADUATE SCHOOL OF SCIENCE ENGINEERING AND TECHNOLOGY** student ID 504111063, successfully defended the **thesis** entitled "**Design of New Type High Efficiency Magnetic Gear**", which he prepared after fulfilling the requirements specified in the associated legislations, before the jury whose signatures are below.

Thesis Advisor :	**Asst. Prof. Dr. Fuat Küçük** Istanbul Technical University	.....
Jury Members :	**Assoc. Prof. Dr. Lale Tükenmez Ergene** Istanbul Technical University	.....
	Asst. Prof. Dr. Metin Aydın Kocaeli University	.....

Date of Submission : 28 April 2015
Date of Defense : 28 May 2015

FOREWORD

I sincerely thank to my supervisor, Asst. Prof. Dr. Fuat Küçük, for guidance, helping and encouragement in carrying out this project work. Also, I wish to avail myself of this opportunity, express a sense of gratitude and love to my kind parents for their support, strength, help and for everything.

May 2015

Sadra Mousavi

Electrical Engineer

TABLE OF CONTENTS

ABBREVIATIONS

MG	**:** Magnetic Gear
MGPMG	**:** Magnetically Geared Permanent Magnet Generator
PM	**:** Permanent Magnet
E-CVT	**:** Electric Continuous Variable Transmission
FEA	**:** Finite Element Analysis
TPME	**:** Tripple Permanent Magnet Excited
EMF	**:** Electro Motive Force

LIST OF TABLES

Page

LIST OF FIGURES

Page

DESIGN OF NEW TYPE HIGH EFFICIENCY MAGNETIC GEAR

SUMMARY

In the field of electric machine design, increasing torque density and efficiency is one of important aims. When machines fail to meet torque density requirements or are simply incapable of matching load torque, gears are commonly used. Gears are used abundantly in industry, because they can change speed and torque according to application requirements. However, mechanical gears have some disadvantages such as acoustic noise, high cost of maintenance, frequently maintenance needed and also low reliability. Consequently, Magnetic Gears (MG) have been proposed as a means of increasing torque density within electromechanical systems, while avoiding problems associated with traditional mechanical gears.

Magnetic gears have many advantages in comparison with mechanical gears that will be discussed in following sections. In this thesis, a newly configured magnetic gear will be proposed which has higher torque capability and better efficiency in compared with other magnetic gears. In the first chapter, a brief introduction is given and history of magnetic gear will be explained, also, objectives of using magnetic gears will be discussed. Then background knowledge about gears which can help us to have better understanding about principles of magnetic gears will be presented. In the second chapter, mathematical computation and formulation of flux generation in magnetic gear will be explained. Moreover, equivalent circuit of Magnetically Geared Permanent Magnet Generator (MGPMG) will be explained. In the third chapter, design technics, simulation results of newly configured magnetic gear with new capability and also efficiency analyses will be presented. First of all, analyses which have been done on conventional form are presented. Then, proposed configuration will be introduced, additionally; result of static, steady state and transient analyses will be presented. Lastly, result of efficiency calculations and comparison will be given also in this chapter. In the last chapter, new and recommended ideas which are better to be done in further works is discussed.

YÜKSEK VERİMLİ MANYETİK DİŞLİ KUTUSU TASARIMI

ÖZET

Elektrik makinelerinin tasarımında moment/hacim veya güç/hacim oranının yüksek olması beklenir. Elektrik makinaları, yük momentini karşılamada yetersiz kaldıklarında ara eleman olarak dişliler kullanılır. Sanayide yoğun olarak kullanılan dişliler momenti veya hızı belli oranda arttırabilir veya azaltabililler. Böylece elektrik makinesiyle yük arasındaki dengeyi sağlarlar. Mekanik dişliler akustik gürültüsü, sıkça yağlama ve bakım gerektirmesi ve aynı zamanda bakım maliyetinin yüksek olması gibi dezavantajlara sahiptir. Manyetik dişliler ise dişliler arasında fiziksel temas olmadığından hem sessiz çalışırlar hem de yağlama ve bakım gerektirmezler. Maynetik dişliler klasik dişlilere göre daha yüksek güç/hacim oranına sahiptir, dolayısıyla mekanik dişlilere iyi bir alternatif . olma potansiyeline sahiptir.

Manyetik dişliler birden çok tasarımlara sahiptir; bunlara örnek olarak yüzeysel mıknatıslı, spur, planetary, spoke tipleri verilebilir. Bunlardan en çok bilineni yüzey mıknatıslı manyetik dişlilerdir. Manyetik dişlilerde farklı çeşitte mıknatıslar kullanılmaktadır. Bunlar arasında Neodyum-Demir-Bor (NdFeB), Samarium Kobalt(SmCo) ve Alüminyım-Nikel-Kobalt (Alnico) sayılabilir. NdFeB mıknatıslar hem yüksek akı sağlaması hem de ters manyetik alana dayanma kabiliyeti çok iyi olması nedenleriyle elektrik makinelerinin tasarımında sıklıkla kullanılırlar. SmCo mıknatıslarının en belirgin özelliği ise sıcaklık arttışına karşı performanslarını koruyabilmeleridir. Fakat NdFeB'lardan pahalıdırlar. Bundan dolayı askeri ve tıbbi sanayinin özel uygulamalarında kullanılırlar. Alnico ticari bakımdan en eski mıknatıslardan biridir ve manyetik çeliklerin ilk versiyonlarından geliştirilmişlerdir. İçeriğinde barındırdığı ilk elementler: isminden anlaşıldığı gibi; alüminyum (Al), nikel (Ni) ve kobalt (Co) elementleridir. Kalıcı mıknatısiyetleri yüksek olmasına karşın, görece düşük akı değerlerine sahiptirler ve en büyük dezavantajları kolayca demanyetize olmalarıdır. Fakat, ısıya dirençlidirler ve iyi mekaniki özelliklere sahiptirler.

Klasik manyetik dişliler üç adet dönebilen kısmdan oluşmaktadır. İki parçası hareketli ve bir parçası sabittir. Hareketli kısma rotor ve sabit olan kısma stator denir. Bazı uygulamalarda, dış kısım stator görevini görürken orta kısm ve iç kısım rotor görevini görür. Diğer uygulamalarda ise orta kısım sabit tutulurken iç ve dış kısımlar döndürülür. Bu tezde, manyetik dişlilerin kullanılagelen klasik konfigürasyonlarına nazaran daha yüksek moment ve verim elde edilebilen yeni bir manyetik dişli konfigürasyonu önerilmiş ve analizi yapılmıştır.

Birinci bölümde, giriş yapmakla birlikte manyetik dişlinin tarihi başlangıcından günümüze kadar incelenmiştir. Manyetik dişlilerin gelişmesinde ve yaygınlaşmasında etkin rolü olan çalışmalar ve yayınlar değerlendirmiştir. Yine bu bölümde, bu çalışmanın yapılmasındaki amaç ve hedeflerden bahsedilmiştir. Buna ek olarak, birinci bölümün son kısmında, proje boyunca kullanılan analiz programı tanıtılmıştır.

İkinci bölümde, manyetik dişliler ile ilgili matematiksel eşitlikler ve parametrelerin anlamları verilmiştir. Daha sonra, manyetik dişlilerin modellenmesinde kullanılabilecek basit eşdeğer devre açıklanmıştır. Genel olarak manyetik dişlinin rotorlarındaki toplam çift kutup sayısı statordaki kutup sayısına eşit alınır.

Üçüncü bölümde, farklı konfigürasyonların tasarım kriterleri, simulasyon şartları ve sonuçları sunulmuştur. Öncelikle klasik manyetik dişli olarak kabul edilen yüzeysel mıknatıslı manyetik dişlinin geometrik ve manyetik özellikleri referans bir kaynaktan elde edilmiş ve statik analizi yapılmıştır. Statik analizde rotorun biri sabit bir hızda döndürülürken diğer rotor hareketsiz bırakılır. Moment grafiği sinüs şeklindedir. Statik analiz tamamlandıktan sonra sonuçlar referans kaynaktaki sonuçlar ile karşılaştırılmştır. Sonuçların tutarlı olduğu görülmüştür. İkinci aşama olarak yüzeysel mıknatıslı manyetik dişlinin analiz sonuçları referans kabul edilip farklı konfgürasyonlar ile elde edilebilecek iyileştirmeler araştırılmıştır. Farklı konfigürasyonlar denenirken mıknatıs hacminin aynı kalmasına dikkat edilmiştir. Elde edilen sonuçlara göre V şeklinde gömülü mıknatıslı manyetik dişli klasik manyetik dişliye göre en yüksek momenti sağlamıştır. Statik analiz sonuçlarına göre momentte %9.5'luk bir artış sağlanmıştır. Daha sonra yeni konfigürasyonun kararlı ve geçici hal analizi yapılmıştır. Kararlı hal analinde iç ve dış rotor çevirme oranına göre belirlenen hızlarda döndürülerek elde edilir. Geçici hal analizinde ise manyetik dişlinin rotorlarından birine yük bağlanarak yapılmıştır. Diğer rotor belirli bir hızda döndürüldüğünde yükün bağlı olduğu rotorun hızına bakılır. Böylelikle yük, eylemsizlik ve sönümleme katsayısının manyetik dişli davranışına etkisi incelenir. Yapılan anlizde moment ve hız başlangıçta osilasyon yapsa bile yük momenti, eylemsizlik ve sönümleme katsayısına göre belirli bir değere oturmuştur. Gerek kararlı hal gerekse de farklı yüklerde için yapılan geçici hal analiz sonuçları tutarlı bulunmuştur. Çevirme oranı her iki durumda da teorik çevirme oranı olan 5.5'a yakın bulunmuştur. Sonraki analizlerde, yeni tip (IPM) manyetik dişlinin analizlerine geçilecek ve farklı yüklerde elde edilen analiz sonuçları verilecektir. Son olarak V şeklinde gömülü mıknatıslı manyetik dişlinin verimlilik analizleri yapılmıştır ve klasik manyetik dişli ile karşılaştırılmıştır. Bunun için kararlı hal analizinden yararlanılmıştır. Verim analizinde histerezis ve girdap akımı kayıpları hesaba katılırken kayıpların hıza bağlı olarak nasıl değiştiği araştırılmıştır.

Son bölümde ise sayısal sonuçlar değerlendirilmiş ve ilerde yapılacak çalışmalar için bazi onerilerde bulunulmuştur. Elde edilen sonuçlara göre V şeklinde gömülü mıknatıslı manyetik dişli klasik manyetik dişliye göre herhangi bir maliyet artışına neden olmamıştır. Önerilen manyetik dişlinin verimi çevirme oranı 5,5 kalacak şekilde belirlenen üç faklı hız için hesaplanmıştır. Elde edilen sonuçlar incelendiğinde, klasik manyetik dişli verimine göre 60/330 min^{-1} de %2'lik bir artış, 1200/6600 min^{-1} de %6'lık bir artış, % 2400/13200 min^{-1} de ise %15'lik bir artış sağlanmıştır.

Önerilen yeni konfigürasyon özellikle yenilenebilir enerji kaynaklarından olan rüzgar enerjisi dönüşüm sistemleri için uygundur. Çünkü rüzgar hızı genellikle generatörün (özellikle asenkron generatör) anma hızına göre düşüktür ve dolayısıyla generatör verimli çalışabilmesi için dişli kutusu gereklidir. Manyetik dişlilerin mekanik dişlilere göre zaten mevcut olan pek çok avantajın yanısıra ve önerilen konfigürasyonun veriminin 1500 min^{-1} de %90 civarı olması önemli bir gelişmedir. Bu da önerilen konfigürasyonun rüzgar türbinlerinde kullanılagelen mekanik dişlilere iyi bir alternatif olabileceğini göstermektedir. Bu çalışma daha sonra yapılması planlanan manyetik dişli gömülü motor/generatör çalışmalarına önayak olacaktır.

Manyetik dişli ile sürekli mıknatıslı generatörü ayrı ayrı kullanmak yerine birleştirilerek hem maliyet azaltılabilecek hem de yerden tasarruf sağlanabilecektir. Böylece rüzgar türbinlerinin yaygınlaşmasına ve termik santrallerin neden olduğu hava kirliliğinin azaltılmasına katkıda bulunulabileceği düşünülmektedir.

1. INTRODUCTION

Gears have been extensively used in all kinds of industrial applications, for transmitting torque and adjusting speeds. So far, a mechanical gear which involves two or more metal discs meshed with each other through the teeth at their rims is still the leading player in this role. However, because of its contact mechanism, the associated transmission loss, noise, vibration, and thus regular lubrication are inevitable. With the advent of high-energy permanent magnet (PM) material, the concept of non-contact torque transmission through the interaction between PMs has attracted increasing attention. Consequently, a PM based non-contact gear is so-called the magnetic gear. Gears are mostly used in industry such as wind turbines and the most important part of wind turbine, which captures wind energy in order to convert it to electrical energy, is gear. Magnetic gears (MG) have lots of advantages over their mechanical counter parts such as reduced maintenance and improved reliability, inherent overload protection, physical isolation between the input and output shafts and low rate of noise. These advantages encourage scientists and producers to replace mechanical gears with magnetic gears.

1.1 History of Magnetic Gear and Literature Review

Magnetic gearing can be traced back to the 20th century. Armstrong [1] designed an electromagnetic spur gear in 1901. The gear consisted of two gears, one with electromagnets as the gear teeth and the other with steel pieces. The electromagnets on the primary gear were switched on and off according to their relative position to the secondary gear teeth. An illustration can be seen in Figure 1.1. The gear had the advantage of contact-less power transfer and low noise operation, but fell short in the amount of torque that could be transferred for the volume occupied. Only one to three electromagnets transferred torque at any given moment. The electromagnets had to be connected electrically with slip rings, which caused unnecessary losses and needed high maintenance.

In 1916 Neuland [2] invented a far superior magnetic gear. The gear consisted of three main parts, a laminated steel outer- and inner-rotor and magnetic modulation pieces in between the two steel rotors (see Figure 1.2). The modulation pieces were shaped to modulate magnetic flux so that the inner rotor and the outer rotor saw the correct harmonics in accordance with the number of teeth on each shaft. The ratio of teeth on the outer- and inner-rotor determined the gear ratio between the shafts. The torque density of this configuration was greatly improved compared to the spur-type design from [1], since most of the gear teeth transferred torque at any given moment. The patent also described a few variations on the design. The problem with this design was that there were only magnets on one of the shafts, which led to impractical air-gap sizes.

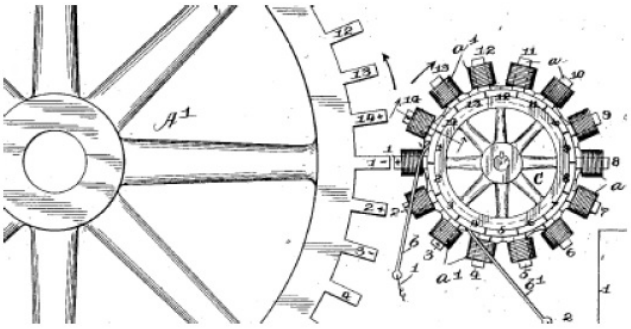

Figure 1.1: First magnetic gear [1].

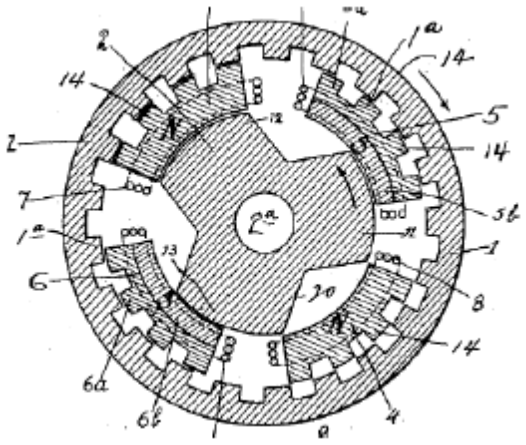

Figure 1.2: Coaxial magnetic gear [2].

Zweigbergk (2) designed an electromagnetic gear in 1919. The machine was known as Electric-Continuous-Variable-Transmission (or E-CVT). E-CVT was basically two electrical machines joined together; one motor and one generator. The generator

acted as the input and the electricity generated drove the motor, the motor was the output. The advantage of the machine described was that the output speed of the motor could be controlled; hence continuous variable transmission could be obtained. CVT could be very advantageous especially in renewable energy applications. If constant output speed could be maintained the power electronics controlling the generated electricity quality could be reduced to a simple system. The disadvantage of this E-CVT was that two machines were needed, which doubled the amount of magnetic and electrical materials needed and most likely one of the machines would need slip rings. The efficiency of the system would then be the combined efficiency of the individual systems.

H.T. Faus designed a magnetic spur-type gear in 1941, [4]. The gear operated in the same manner as the electromagnetic spur gear from (1) as described above. The only difference was that it used permanent magnets (Figure 1.3 illustrates the original design from the patent). All the north poles of the magnets pointed radially outwards, thus the torque was transferred between the shafts by the repulsion of the identical poles of the magnets. When the maximum torque was exceeded in this design the gear slipped and caused one of the permanent magnets to break, since the PMs still made contact. Thus this design was not suitable when overload protection was necessary. Although it improved on the previous spur-type designs by eliminating the electromagnets, which decreased the weight and the size of the gear while making the control circuit dispensable, the weak utilization of the PMs in the spur-type design made the design impractical. In the patent a worm-type gear was also described.

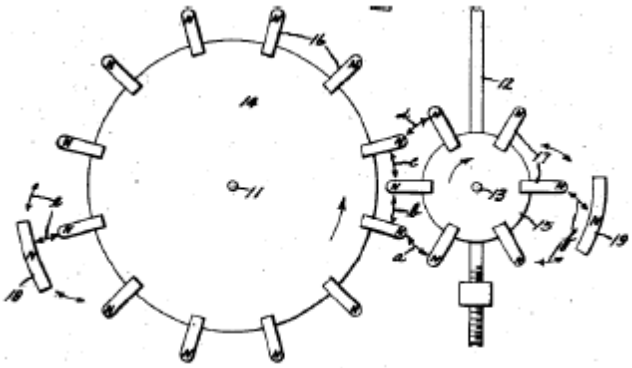

Figure 1.3: Permanent magnet spur type gear [4].

In 1901 when Armstrong [1] designed his gear, PMs were not yet strong enough for efficient gearing, but as the PM technology improved, more and more PM gears appeared. In 1951 Hurvitz [20] invented a spur-type magnetic gearbox, where the gear ratio could be changed by switching the active gears by means of electromagnets. The whole system was not efficient and very bulky. In 1955 Cluwen's patent [21] described a number of spur-type magnetic gear arrangements from normal spur gear arrangements to gearbox arrangements where the gear ratio could be changed by means of moving the driven shaft mechanically to a new position. The patent also described gear arrangements where the axes of rotation were at an angle to one another. In 1966 Baermann [22] invented a device for electricity generation. The device was a belt and pulley system made of permanent magnets (see Figure 1.4). The belt was then moved past electric coils, where the moving magnets induced an electric current in the coils. The movement of the belt was accomplished by the magnetic attraction between the poles on the belt and the pulleys.

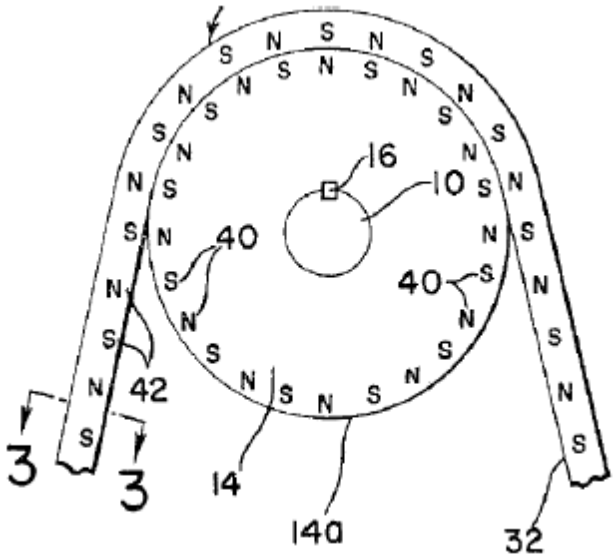

Figure 1.4: Belt and pulley permanent magnet device [22].

In 1967 Reese [23] invented a magnetic gear similar to the one described in [2]. The difference was that the inner rotor contained the PMs (see Figure 1.5 for an illustration of the gear). The two outer rotors had a different number of teeth. The inner PM-rotor was the high speed shaft, the middle rotor was the output shaft and the outer rotor was kept stationary. When the inner PMs were rotated, the middle

rotor would rotate with it. The magnetic flux of the PM's tended to take the path with the lowest permeability, which is through the steel teeth of the rotors. This made the teeth of the rotor rotate in accordance with the magnetic flux of the PMs. The speed of the rotor then became a function of the ratio of the number of teeth between the rotors and the number of PM poles.

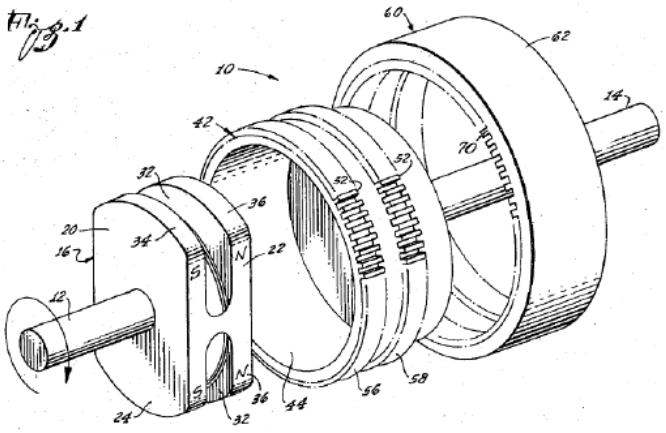

Figure 1.5: Coaxial magnetic gear [23].

In 1970 Rand [24] took out a patent for a simple spur-type magnetic gear. He designed the PMs so that both the north and south poles of the PMs faced radially outward (see Figure 1.6). This increased the amount of magnetic material needed and the cost of manufacturing. In 1972 Laing [25] took out a patent for a magnetic gear that the flux-modulator in between the PM rotors were a bit different and that only every second pole on the rotors contained a PM (see Figure 1.7). In 1973 Laing took out another patent, [26], this patent described the magnetic gear incorporated into a centrifugal pump. The advantage of using a magnetic gear in a pump is that the two rotating shafts transferred torque without physical contact, thus the pump could be sealed.

In 1980s, with the advent of rare-earth permanent magnets (PMs), such as Neodymium-Iron-Boron (NdFeB) magnet [5], the concept of magnetic gears began to attract people's attention again. Rare-earth PMs has the ability to produce very strong magnetic field without continuous exterior excitement. Early work was done by Tsurumoto [6-7] with non-concentric magnetic gears using Samarium Cobalt magnets. More research and prototypes followed with the concentric planetary magnetic gear in [8],[9], and [10].

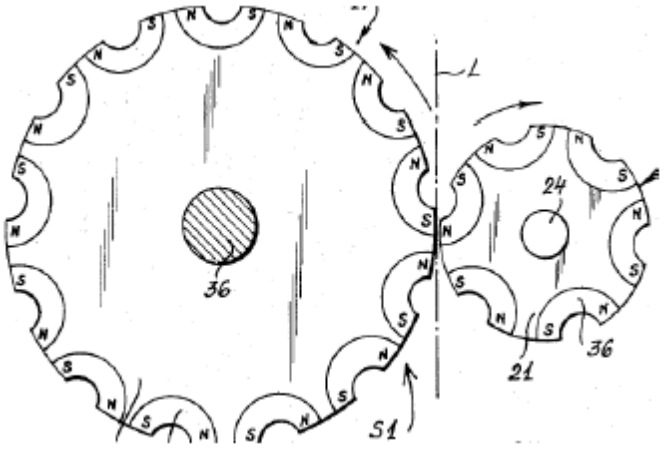

Figure 1.6: Spur-type magnetic gear with U-magnets [24].

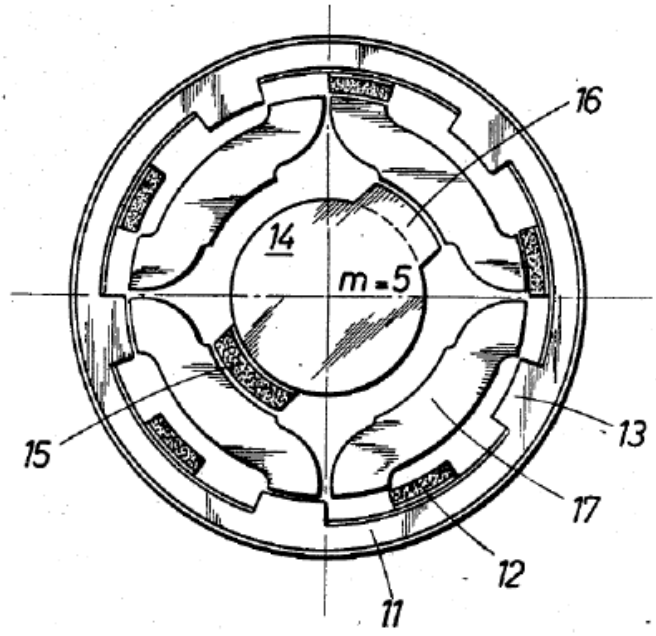

Figure 1.7: Coaxial magnetic gear used in [25].

Hesmondhalgh et al.(1980) [27] proposed an array of Neuland's [2] magnetic gears (see Figure 1.8), in a hope that the array of gears would increase the maximum torque and efficiency and reduced the cogging torque. However, the total efficiency for the system was very low and the combined gears made the whole system too large and complex.

K. Tsurumoto was the inventor of the axial flux disk type spur magnetic gear (see Figure 1.9). In 1987 Tsurumoto [6] published his first paper on the non-contact

magnetic gear. The permanent magnet material used was samarium-cobalt. The gear had a gear ratio of 1/3. The maximum torque that could be transferred was 5.5 Nm. In 1988 he described an attempt to improve the performance of the gear by mounting the magnets directly on a soft steel plate or a yoke [7]. His conclusion was that identical gears could be used for both internal and external meshing.

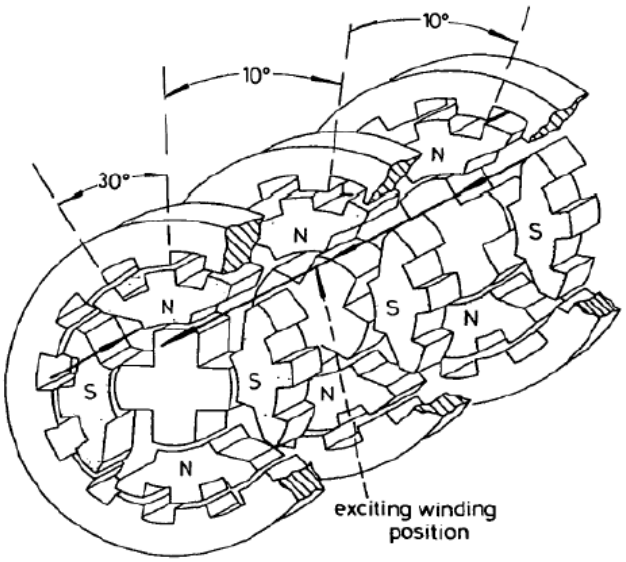

Figure 1.8: A multi-element magnetic gear [27].

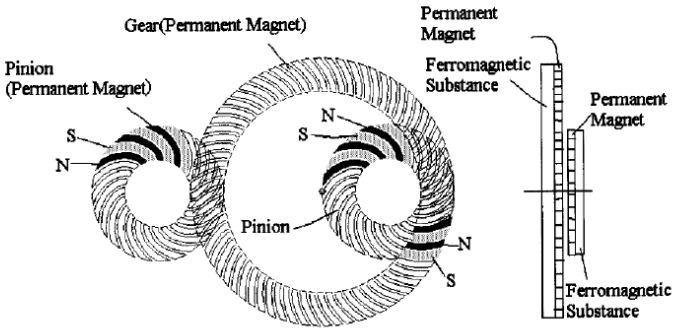

Figure 1.9: Axial-flux disk-type spur magnetic gear [6].

The next paper was published in 1989, [29], it expanded on the previous article and concluded that the output torque could be 3.2 times improved if the magnets were placed on yokes. Tsurumoto published another paper in 1990, [30], in which he described the design and overlap area of PM's and the performance characteristics of circular arc magnetic gears. He concluded that circular arc magnetic gears are 6%

more efficient than those in his original design. The efficiency increase was due to the extra PM material in the meshing area.

In [31] Tsurumoto investigated the mechanism by which magnetic force was generated in the meshing area of the two opposing rotors. In 1992 he wrote a paper [32] about using a two-dimensional model was used an approximation of the generated magnetic force between the main contacting and intersecting zones of a magnetic gear using permanent magnets.

An interesting paper [33] was written in 2002 that described a superconducting axial flux magnetic gear. Superconducting magnets can be several times stronger than rare earth magnets. However this required constant refrigeration which increased the total size and mass. The author also described the development of a three dimensional electromagnetic field analysis program to analyses characteristics of the proposed gear. Two superconducting magnetic gears with different configurations were manufactured and tested. The test results did not show good agreement with the calculated results, due to scatter in the experimental results. Superconducting magnetic gears could greatly improve the maximum torque that can be transferred when compared to normal permanent magnetic gears.

In the next paper [34] a magnetic worm gear was described (1993). The proposed gear has a gear ratio of 1:33. The original design had a low maximum torque capability, due to a large air-gap. The airgap was then decreased by mating the worm gear with the wheel (as can be seen in Figure 1.10) and the output torque increased by about 1.5 times. However, the intricate parts increased the fabrication and assembly costs. The magnetic worm gear was feasible but the complexity and the costs of manufacturing were only worthwhile in applications where the advantages of magnetic gears were necessary.

Magnetic skew gears were discussed in [35,36]. The gear consisted of two worm mates and no wheel gear. Thus only a small magnetic area was responsible for the transfer of torque at any given moment. This design was worse than the design of 1993 because of the small area that could be used to transfer power, but the fabrication cost was decreased.

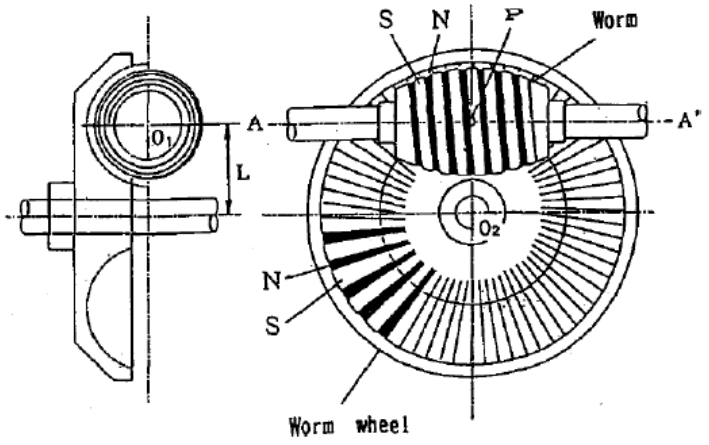

Figure 1.10: Magnetic worm gear [34].

In 1996 a paper, [37], was published where a perpendicular magnetic gear was designed, built and experimentally evaluated (an illustration of the proposed gear can be seen in Figure 1.11). The paper described a critical separation distance (d in Figure 1.11) where if the air-gap length was smaller than the critical distance the transmitted torque could be increased by increasing the number of poles.

Yao et al. (from 1996 to 1997) described the coupling between spur-type magnetic gears. The first paper, [38], described the coupling of spur-type magnetic gears with both two- and three-dimensional finite element analysis (FEA). The conclusion was that for a 2mm air-gap the torque could be increased by increasing the number of poles. The torque was inversely proportional to the number of poles when the number of poles was larger than ten.

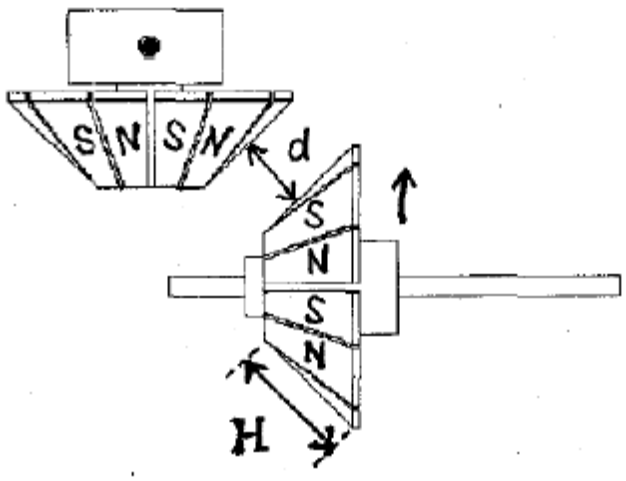

Figure 1.11: Perpendicular magnetic gear [37].

In the next paper [39] the optimization conclusions of a 2D FEA simulation were described. It was concluded that with a fixed air-gap distance a maximum torque could be obtained for a particular number of poles. The number of poles increased as the ratio of the radius to the thickness of the magnets increased. The number of poles decreased when an iron yoke was added. In the following paper [45] the authors attempted to prove the conclusions made in the previous two papers by experimental testing. Furlani [41] presented a formula to calculate the coupling between spur-type magnetic gears in 1997. The formula was based on two-dimensional analytical analysis and it was expressed as a finite sum of elementary functions. The formula was demonstrated practically and was verified using 2D FEA. The formula was ideal for parametric analysis.

Atallah et al. (2001) wrote a paper [8] on a "novel" magnetic gear. The gear was fundamentally the same as Ackerman's 1997 gear, except that the flux-modulator was not connected (see Figure 1.12). In the paper the relationship between the number of poles and the number of modulation pieces in the gear were described to determine the gear ratio. It was claimed that by using rare earth magnets a torque density exceeding 100 kNm/m3 could be achieved.

In 2003 Rasmussen wrote a paper [9], on a coaxial magnetic gear, the same as described above, except that the inner rotor's magnets were arranged in a spoke-type arrangement and not surface mounted (see Figure 1.13). It was calculated that the gear would have a gear ratio of 1:5.5 and a stall torque of 27 Nm. However, the experimental results showed a stall torque of only 16 Nm. The reduction in the stall

torque seemed to be caused by the end-effects of the short stack length of the magnets. In the paper MG is also compared with conventional mechanical gears with the same gear ratio and maximum torque capabilities. It was concluded that a theoretical efficiency of 96% could be reached if the end-effect losses were minimized and the gear had a higher torque density when compared to other mechanical gears.

In 2004 Atallah et al. [28] improved their previous paper on coaxial magnetic gears by demonstrating that an efficiency of 97% could be reached for transmitted torque values higher than 75% of the pull-out torque.

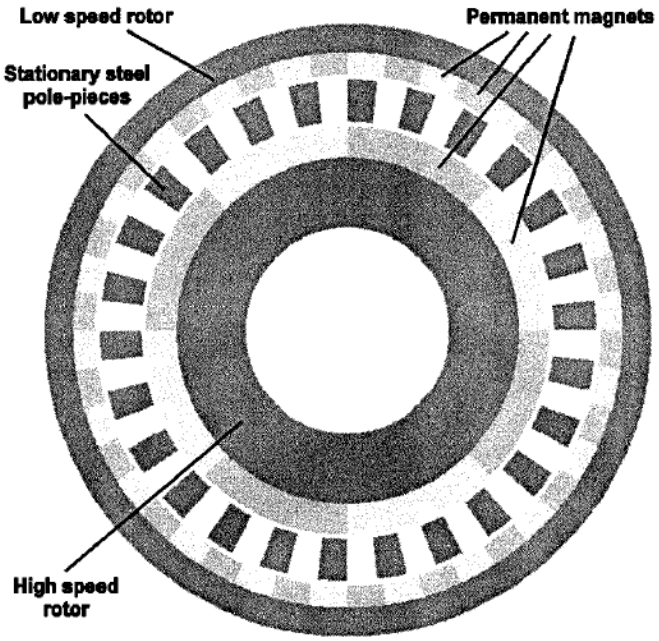

Figure 1.12: Coaxial magnetic gear [8].

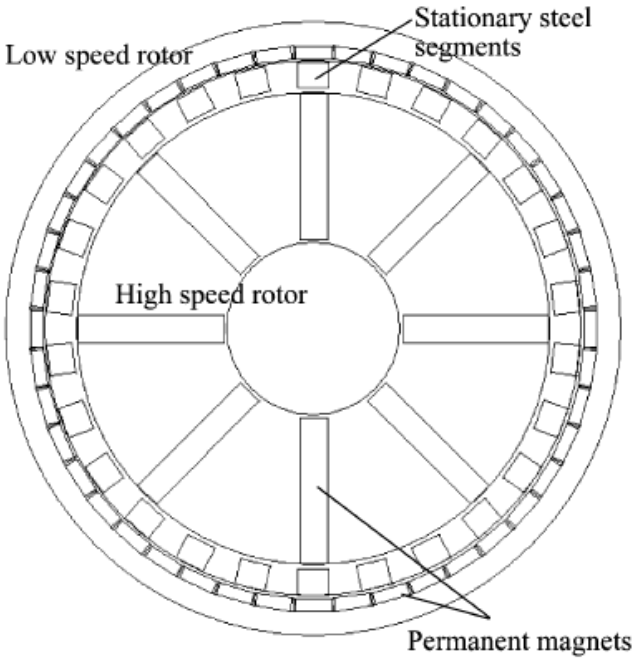

Figure 1.13: Coaxial magnetic gear with spoke type of PMs on inner rotor [9].

Atallah et al. 2005 published a paper [42] on a linear magnetic gear. The gear operated on the same principle as the coaxial magnetic gear. There were three parts that moved relative to each other: two PM armatures connected to steel yokes and one flux-modulator core. The flux-modulator core modulated the magnetic flux

between the inner and outer PM armatures, so that the PM yokes interacted with the correct number of poles (correct space harmonics). The proposed linear gear was simulated and the results showed that a thrust force of 1.7 MN/m3 could be obtained. It was also shown that a linear magnetic gear combined with a linear electrical machine could obtain a high force density, even with a relatively low gear ratio.

In [10], windings were placed on the outside of the concentric planetary magnetic gear to help dampen the gearbox against transient responses. In 2007 an interesting paper, [11] surfaced, in which the experimental results for the application of a coaxial magnetic gearbox being used in a contra-rotating tidal turbine were described. The contra-rotating tidal turbine comprised of two sets of blades; the upstream blade rotated in a clockwise direction whilst the downstream blade rotated in an anti-clockwise direction. The upstream blade was connected to the low speed outer rotor and the downstream blade was connected to the flux-modulator of the coaxial magnetic gear. The coaxial magnetic gearbox combined the output of both contra-rotating shafts into a single high speed rotating shaft (inner rotor). A complete prototype with the blades needed to be constructed in order to test the system. In the same year he wrote another paper, [12], in which two coaxial magnetic gears were compared with each other one with radially magnetized PM's and the other with halbach magnetized PM's. Analysis showed that the halbach magnetized PM's could offer higher pull-out torque, lower torque ripple and lower iron losses than the radially magnetized PM's. In [13], a concentric planetary magnetic gear was built which used an axial flux configuration for the stator pole pieces, instead of a radial flux configuration.

Other designs have also begun to appear to achieve higher torque density ratings. Haung et al. 2008 wrote a detailed paper, [14], on a magnetic planetary gear. The gear arrangement had a sun, planets and a ring-gear very similar to conventional mechanical planetary gears. The difference was that every tooth was replaced with a PM. The maximum torque could be increased by increasing the number of planets, but by increasing the number of planets the cogging torque would also be increased. The constructed gearbox exhibited a maximum torque density of 100 kNm/m3.

In [16] the harmonic magnetic gear was studied and built. In this design, instead of using a cycloid action to modulate the air gap between the magnetic rings, a flexible

rotor was proposed, in which the inner rotor would change shape and thus the air gap.

Rens et al. [43] 2007 proposed a harmonic magnetic gear. The operating principle of the proposed gear was similar to that of a mechanical harmonic gear (see Figure 1.14). The operating principle of a harmonic gear was that a high speed input on the wave generator caused gear teeth on the flexible spline (input) to engage with internal teeth on the circular-spline (output). Since the flexible-spline had two teeth fewer than the circular-spline, each revolution of the input caused a two-tooth displacement of the output. (Figure 1.14B shows a magnetic version of the harmonic gear). For the magnetic harmonic gear the high speed rotor deformed the flexible low speed rotor which rotated within the rigid outer stator. The time varying sinusoidal variation of the air gap length modulated the field produced by the magnets on the low speed rotor and resulted in a dominant asynchronous space harmonic field which interacted with the magnets on the stator to facilitate torque transmission and the magnetic gear action.

The harmonic gear was further complicated by the need for a flexible permanent magnet low speed rotor assembly. One way to simplify the design and make it more practical, was to use a rigid low speed rotor which was driven eccentrically by the high speed rotor so that a single cyclic variation of the air gap resulted between the permanent magnets on the low speed rotor and the stator (see Figure 1.15). This version was far better than the flexible version (as can be seen in 1.14B) but not without complexities.

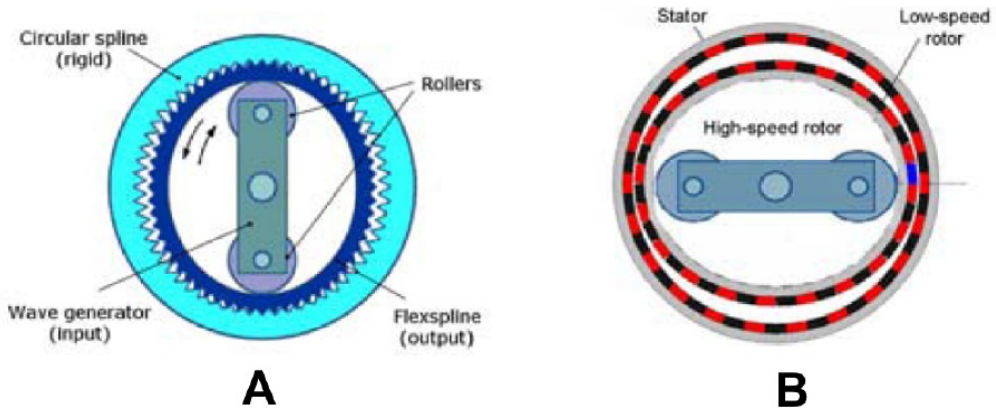

Figure 1.14: A) Mechanical harmonic gear. B) Magnetic harmonic gear [43].

The problem with this design is that the rigid low speed rotor rotated eccentrically; the output shaft needed to be connected with this eccentrically moving rigid low speed rotor and this could only be done with a flexible coupling or with two bearings one inside the other but with the same eccentric distance apart. (Figure 1.16 shows the cycloidal bearings with the eccentric distance between the bearings). Another problem associated with the eccentric distance is that an unbalanced magnetic force was generated because one side of the high speed rotor was always closer to the low speed rotor (the varying air gap).

Figure 1.15: More practical harmonic magnetic gear [43].

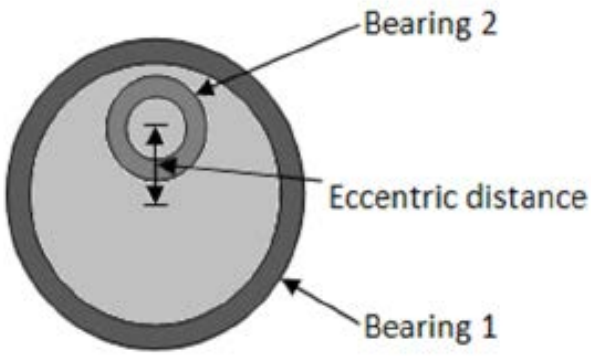

Figure 1.16: Cycloidal bearing.

Rens et al. 2007, [43] proposed a dual stage magnetic harmonic gear (see Figure 1.17). This eliminated the need for a flexible coupling and further increased the gear

ratio. It was shown in the paper that a dual stage harmonic gearbox could obtain very high gear ratios. Torque densities of up to 110 kNm/m3 could be achieved and the transmitted torque exhibited no torque ripple. Finally the dual stage harmonic magnetic gear exhibited a higher gear ratio than the product of the ratios of the individual stages.

In 2008 Jorgensen et al. wrote a paper, [15], on a harmonic gear with two identical stages. The second stage was placed so that the unbalanced force of the varying air-gap of the first stage was cancelled by the unbalanced force of the second stage. The problem with this arrangement was that the cycloid motion of the two stages needed to be transferred from the one to the other stage and to the output shaft. The problem was solved by employing cycloidal bearings (see Figure 1.16). However, 12 bearings were needed to solve the cycloid motion, which in turn caused extra losses. Despite all the extra bearings the proposed gearbox succeeded in reaching an efficiency of over 90%.

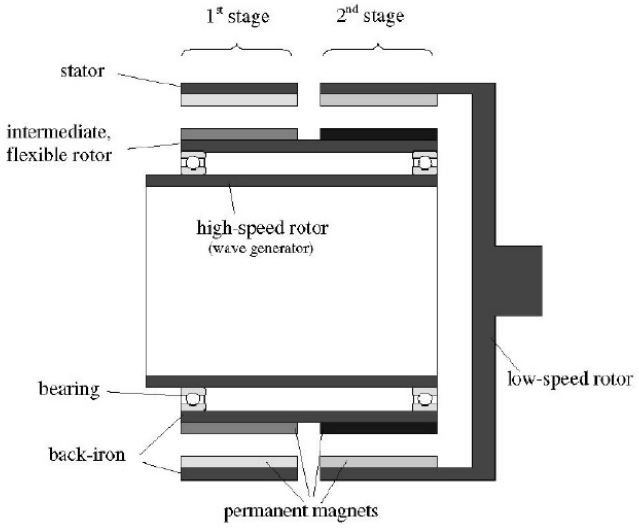

Figure 1.17: Dual stage harmonic magnetic gear [43].

Chau et al. published a paper, [44] about a new integrated design in 2007. The paper described a PM DC brushless motor integrated into a coaxial magnetic gear. The machine was similar to Razzel's design of 2004 (see Figure 1.18). The combined system offered the low speed capabilities of magnetic gears and the high speed requirements for compact motor design, which gave the combined system high torque density and high efficiency at relatively low speeds. The machine was proposed for electrical vehicles. The proposed motor had fractional slot windings

which decreased the cogging torque. The motor without the gearbox had a maximum output torque of 15 Nm, which was insufficient to launch the vehicle. With the gearbox the output torque was increased to 103 Nm, almost 7 times larger, which was sufficient to launch the vehicle.

In 2008 two more papers, [45,46], were written on the design process described above. Jian et al. [46] built a 500 W prototype of the proposed machine. Both the static and dynamic characteristics of the motor have been studied by time-stepping finite element method and Matlab/Simulink. Both the simulation results and the experimental results verified the validity of the proposed motor.

In 2009 Jian et al. [47] proposed the same configuration for use in wind turbine applications. The combined system was ideal for wind power generation. The proposed machine was then compared to a direct drive and a planetary geared PM brushless machines with identical electrical specifications. The proposed topology was of smaller size and lighter weight than both machines, with also lower material cost than the direct driven one.

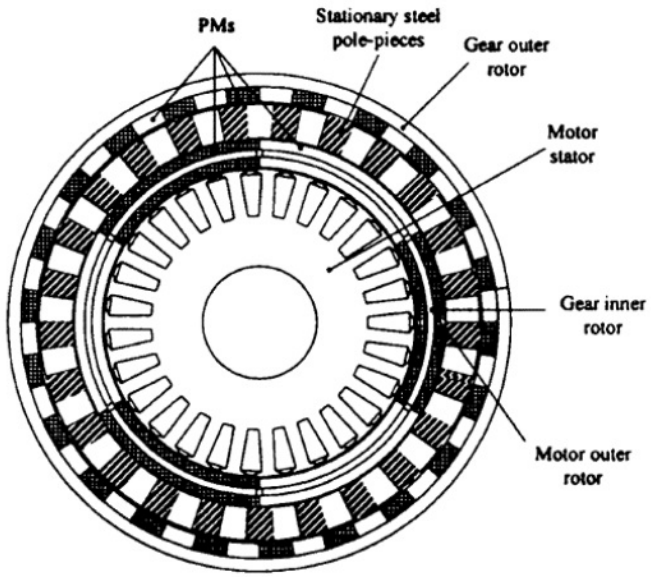

Figure 1.18: Magnetic geared PM machine (with internal stator) [44].

Hafla et al. 2007 wrote a paper [48], on the efficient design analysis of a coaxial magnetic gear on a high performance computer. The emphasis of this paper was on an efficient analysis of a magnetic gear with an integral equation method. For an accurate analysis of a coaxial magnetic gear a non-linear three dimensional analysis was necessary. The analysis required meshing of all the components including the

small air-gaps. By using a fast and efficient matrix compression technique and parallelization the meshing of the air-gaps became unnecessary and this resulted in accurate results along with acceptable computational costs. In the paper there was a description of full numerical analysis of a magnetic gear including saturation effects and the three-dimensional structure with integral equation method and how it could be implemented with parallelization, which was necessary for the efficient use of modern computers.

In 2008 Wang et al. [49] proposed a simplified version of Chau's [44] design of 2007. The proposed machine had no inner rotor (see Figure 1.19). The machine was called a flux modulated permanent magnet machine. The machine operated in the same manner as a coaxial magnetic gear, however the high speed rotary field was produced with an armature rather than by magnets. In 2009 he wrote a similar paper, [50]. In this paper they described the topology and its operating principle. Some techniques were employed to optimize and improve the motor performance, while the validity of the proposed techniques were verified with finite-element analysis. Moreover, an alternative operating condition was proposed and analyzed. This was where the outer rotor was kept stationary and the flux-modulator was rotated. The proposed operating principle further decreased the motor speed, while increasing the output torque.

In 2008 he wrote two more papers about the PSEUDO drives, [51,52]. In both papers the operating principle of magnetically geared brushless machines were described. In both papers it was concluded that the machines could reach torque densities in excess of 60 kNm/m3 and that the machines had a power factor of 0.9 or higher.

Reinap and Marquez published a paper [53] that focused on the design of a linear magnetic gear. The main purpose of the project was to gain analysis skills as well as practical experience of dealing with electromagnetic design for electrical engineering education. In the paper the whole design process was described and an example was given, which makes it ideal for a student with minimal experience in magnetic gears and electromagnetic design.

Davey et al. wrote a general paper [54] on magnetic gears in 2008. The paper described the mainstream magnetic gearboxes and focused on the harmonic magnetic gears. Jong et al. rearranged the coaxial magnetic gear in his paper, [13], of 2008. The proposed gear had the same components as a coaxial magnetic gear, except that

both rotors were internal (see Figure 1.20). The proposed configuration reduced the external diameter of the gear and simplified the mechanical design. The placing of the shafts and supporting bearings had to be considered carefully, so as not to cause unwanted eddy current losses. The paper included an interesting sizing procedure where the influence of the different part sizes was compared in order to determine an optimum design. The configuration could be ideal in applications where the layout is desirable.

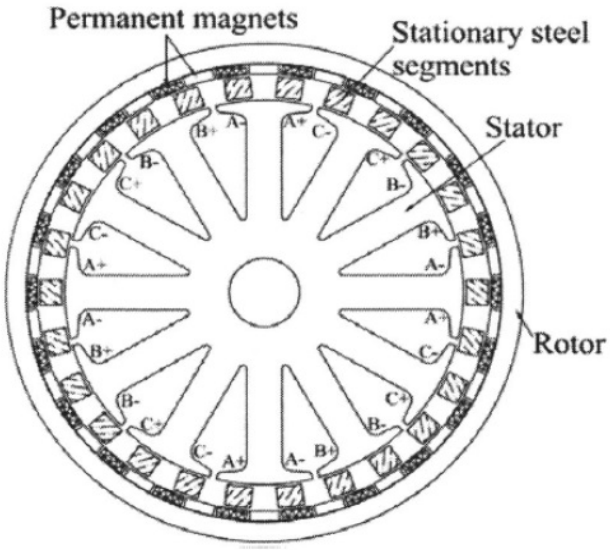

Figure 1.19: Magnetic geared PM brushless machine (no inner rotor) [49].

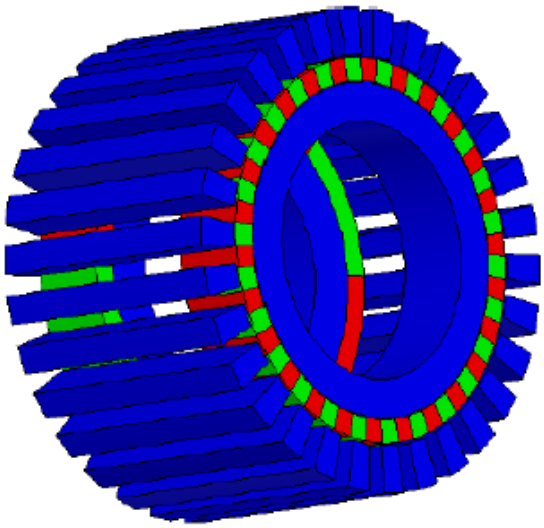

Figure 1.20: Internal high- and low-speed rotors [13].

In 2009 Jian et al. wrote a paper, [55], in which a new analytical approach was proposed to calculate the magnetic field distribution in coaxial magnetic gears. A set of partial differential equations in terms of scalar magnetic potential was used to describe the field behavior, and the solution was determined by considering the boundary constraints. The accuracy of the proposed approach was verified by comparing the field distribution results with those obtained from the finite element method.

Jian et al. then wrote a paper, [56], about the integrated machine with halbach magnetized PM's. The advantage was that the PM motor field and the magnetic gear field were decoupled. In addition, the halbach arrays could enhance the effective harmonic components as well as suppress the unwanted harmonic components of the magnetic field. Other advantages of the halbach array was that maximum torque was increased and iron losses in the outer rotor was decreased. Simulation results based on the time-stepping finite element method were given to verify the validity of the proposal.

Liu et al. wrote a paper, [57], about the coaxial magnetic gear in 2009. In the paper a new topology where the PM's were buried into the iron core of the outer rotor was described. Rather than embedding the alien-polarity PM's into the outer-rotor iron core (as shown in Figure 1.21a) the proposed configuration inserted the PMs with the same polarity into the iron core (as shown in Figure 1.21b). The PM flux flowed in the core bridges equivalently from the alien poles, thus creating a distributed magnetic field with the same number of pole pairs. This improved the mechanical integrity and PM material could be saved while the torque density was maintained. The proposed configuration reduced the magnetic material by 16.5% while decreasing the pull-out torque by only 5.3% for the prototype build.

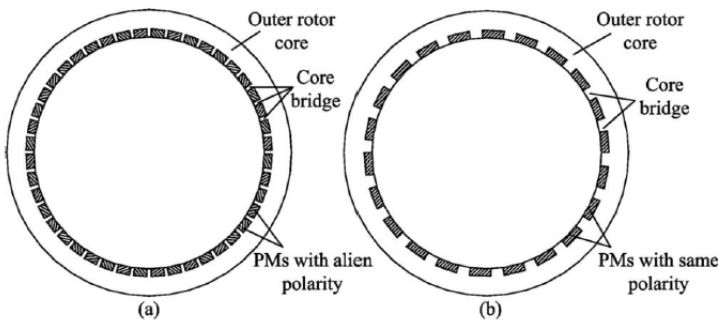

Figure 1.21: Interior PM rotor configurations. a) Traditional. b) Proposed [57].

Frank et al. wrote two papers in 2009, [58,59], in which different applications of coaxial magnetic gears were described. In the first one the use of coaxial magnetic gears for ship propulsion was discussed and in the next one wind power. In both papers the performance of the gear, especially the cogging torque at different gearing ratios was described.

In 2009 Rasmussen et al. published a paper, [60], on a motor integrated magnetic gear similar to the design in [44]. In the previous integrated designs the end windings of the stators were not taken into consideration in the calculation of the torque density. In the proposed design the motor and the gear were carefully designed so that the end windings would not take up extra space. In the paper a scaling process was described in order to determine an optimized gear with the least amount of material and cost. The proposed machine had a maximum torque density of 130 kNm/m3.

Fu et al. in 2010, [61], compared the performance of a flux-modulated PM machine with a magnetically geared PM machine, a traditional PM machine and with a fractional slot PM machine using magnetic field FEA. When comparing the four machines it was necessary to make sure that all motors had the same outside radius and axial length. The motors had the same amount and type of magnetic materials and the same grade of copper and iron materials. The motors also had the same temperature rise at full load. It was concluded that the magnetically-geared motor delivered very large torque at low speeds. The disadvantage was that the machine had too many rotational parts. Compared to the conventional machines the FM-machine had similar torque density. However, the FM-machine had a smaller number of slots and ventilation was better because of the gaps between the modulation pieces. The conventional PM motor had too many slots, its slot area could not be utilized efficiently, the end windings were too long and it also had very large cogging torque. The fractional-slot multi-pole motor had a small number of slots and short end windings. Its output torque was smaller than that of the motor with conventional windings and it had small cogging torque.

In Reference [18] which was published in February 2013 authors introduce the concept of the trans-rotary magnetic gear (that they call it TROMAG). The TROMAG (see Figure 1.22) is a magnetic device consisting of a rotor and a

translator with an air gap in between, capable of converting linear motion to rotation, and vice versa, and doing the gearing action at the same time.

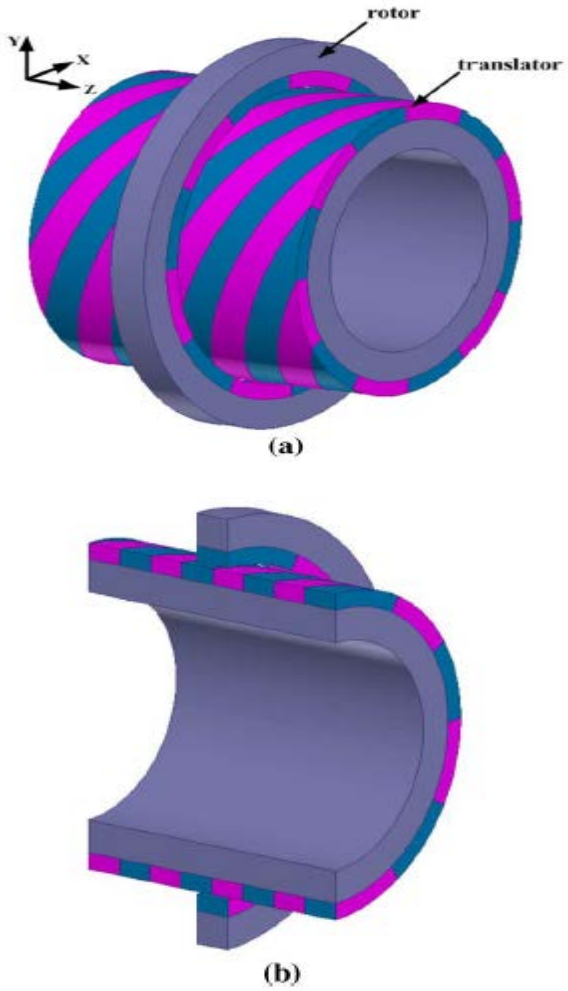

Figure 1.22: (a) 3-D view and (b) cut-away view of a 12-pole TROMAG [18].

Reference [19] proposes a linear permanent magnet (PM) machine for direct-drive wave energy harvesting by using a linear magnetic gear. The proposed machine consists of a linear magnetic gear cascaded with a linear PM generator in which the high-speed mover of the linear magnetic gear and the translator of the PM generator artfully shares with the same shaft. The slow reciprocating wave motion is directly captured by the low-speed mover of the gear, and then amplified in speed via the gear to actuate the generator, hence producing higher output voltage.

Moreover, recently so many researches have been done too. In 2013 and 2014 Jonathan Z. Bird has written papers, [62-64], about coaxial magnetic gears using ferrite magnets.

In [65] author presents a novel triple-permanent-magnet-excited (TPME) hybrid-flux magnetic gear (MG) that integrates a transverse flux MG and an axial-flux MG into a single unit. Compared with its conventional counterparts, the proposed MG transmits a relatively high-torque density. When compared with the transverse-flux MG, this new structure employs a new configuration on the high speed rotor, an extra iron segment between the low-speed rotor and the high-speed rotor to modulate the magnetic field, and hence contributing to the transmission of additional output torque. It also employs permanent magnets on the iron segments to produce additional torque. The proposed TPME hybrid-flux MG can offer a much higher torque transmission capacity than its conventional counterparts, making it more competitive for low-speed high-torque applications.

Reference [66] presents a comparative study between the non-rare-earth PM and rare-earth PM-based coaxial magnetic gear using finite-element analysis. The electromagnetic performances of four coaxial magnetic gears, which are installed with non-rare or rare-earth PMs, are analyzed and quantitatively compared based on the same structure. In this paper the cost effectiveness of coaxial magnetic gears adopting different types of PMs is assessed. The results show that the non-rare-earth PMs, especially the aluminum–nickel–cobalt, are preferred for application to coaxial magnetic gears with emphasis on the cost effectiveness.

In 2014 Yiduan Chen [67] discusses about performances of three types of magnetic gears (MGs), which are radial-flux MGs, transverse-flux MGs, and axial-flux MGs, are quantitatively analyzed and compared. To fairly compare the torque capability of different topologies of MGs, all the MGs under study have the same gear ratio, the same outer diameter, and the same axial stack length. To maximize the torque density, several important structure parameters are optimized. Scenarios using different iron core materials and different magnetization directions of permanent magnets are also studied. Based on the comparative analysis, appropriate topologies of MGs that can achieve a torque density as high as 198 kNm/m3 are suggested.

Reference [68] describes a two-dimensional (2-D) analytical model to predict the magnetic field distribution in axial-field magnetic gears by using the sub-domain

method. The sub-domain method consists in solving the partial differential equations linked to the Maxwell's equations in each rectangular region (magnets, air gaps, and slots) by the separation of variables method.

From the history section it can be observed that magnetic gears are very versatile, MGs can basically be configured in any arrangement that traditional mechanical gears can be configured into. However, MGs offer significant advantages over traditional mechanical gears. Typically, mechanical gears transfer torque with only one to three gear teeth at any given instant, where MG may transfer torque with all of their permanent magnets at any given instant. Thus, MG may occupy a smaller volume and still transfer the same amount of power when compared to mechanical gears.

They offer other advantages as well, such as:

• Power transfer with no contact between parts.

• High gear ratios at a single stage.

• Lubricant free operation.

• Inherent overload protection.

• High torque densities.

• Potential for high efficiency.

• Little or no maintenance.

Two main MG configurations were identified which may offer the most advantages, namely: The coaxial magnetic gear of [2,23] and the harmonic magnetic gear of [43]. Of these two configurations the coaxial MG stands out the most. The harmonic MG have too many complexities that still need to be addressed, such as the unbalanced force of the eccentric rotation. Therefore it was decided that the coaxial magnetic gear would be further investigated.

1.2 Objective

Coaxial magnetic gears are an emerging breed of permanent magnet device which are thought to be a promising substitute for the mechanical gears in all kinds of applications. Although almost ten years have passed since it was firstly proposed,

there are a lot of problems which should be investigated, and this thesis aims to give deep discussions on the following issues:

- Theoretically studying the operating principle of coaxial magnetic gears. As mentioned before, the operation of coaxial magnetic gears lies on the modulating effect aroused from the modulating ring, thus, it is necessary to figure out: firstly, what kind of impacts the modulating ring could make on the magnetic fields, secondly, how come the stable torque transmission is achieved while the two rotors rotating at different speeds, finally, how to further improve the performance of coaxial magnetic gears.
- In this project new configuration of coaxial magnetic gears which has better capability and higher efficiency than other magnetic gears will be proposed. In this new configuration, structure of inner rotor will be developed in order to obtain higher torque and better efficiency, specially, in higher speed situations. Most of experimental works and papers which have been published recently, have some disadvantages such as low rate of torque and low efficiency. Hence, the proposed magnetic gear has improved efficiency and its performance enhanced.
- According to advantages of magnetic gear, which has been discussed in pervious section, using magnetic gears in industry is one of important aims. As an illustration, in wind turbines or cars and etc. Also, in Turkey, there are lots of wind farms and potential for using clean resources in order to generate power. The main part of wind farm is wind turbine and gears plays important role in turbines. Thus, final goal of this thesis is to replace mechanical gears with magnetic gears.

1.3 Background Knowledge About Gears

Although this thesis is devoted to the topics about magnetic gears, for the completeness of understanding, it is necessary to start with a brief introduction on mechanical gears.

As we all know, mechanical gear exists so extensively in industrial applications that it has been thought as the best symbol of modern industrial civilization. In terms of functions, mechanical gears are employed to transmit torques or forces as well as alter the forms of motion, which include the speeds of motion and the directions of

motion. Figure 1.23 shows four typical types of mechanical gears. It can be found that they all consist of several movable parts which are meshed with each other through the teeth at their rims. An important criterion for judging the performance of the mechanical gear is termed torque density, which implies the capability to transmit torque within the unit volume size, namely, the ratio of the maximum torque that can be born to the volume size of the gear. In order to increase the torque density, mechanical engineers have done plenty of work, such as improving the shape of the metal teeth or choosing special steel materials with very high strength.

With different constitutions or shapes, the rules for alternation of motion forms are different. For the spur gear shown in Figure 1.23(a), the rotational speeds of the two metal disks are governed by:

$$\frac{\omega_1}{\omega_2} = -\frac{N_2}{N_1} = -\frac{R_2}{R_1} \tag{1.1}$$

where N_1, N_2, R_1 and R_2 denote the teeth number and the radius of the two metal disks, and the minus notation implies that the two disks should rotate in opposite directions. While for the internal ring gear depicted in Figure 1.23(b), the rotational speeds of the two metal disks is governed by:

$$\frac{\omega_1}{\omega_2} = \frac{N_2}{N_1} = \frac{R_2}{R_1} \tag{1.2}$$

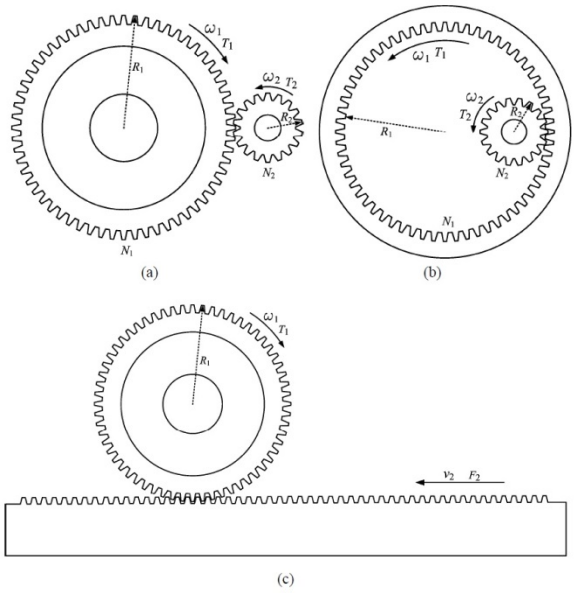

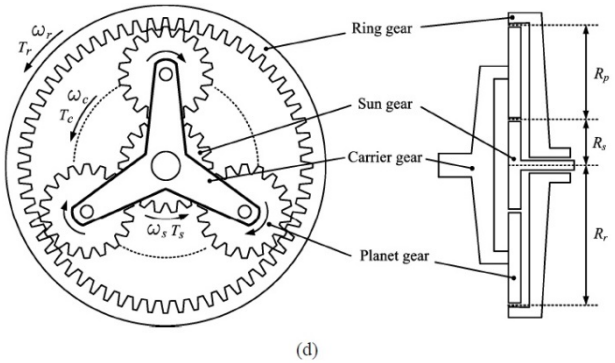

Figure 1.23: Typical types of mechanical gears. (a) Spur gear. (b) Internal ring gear. (c) Rack and pinion. (d) Planetary gear [17].

It means that the two disks should rotate in the same direction. The rack and pinion set given in Figure 1.23 (c) can achieve the transformation between rotational movement and linear movement, which is restricted by:

$$\omega_1 R_1 = v_2 \qquad (\mathbf{1.3})$$

The planetary gear set illustrated in Fig.1.23 (d) possesses the most complicated mechanical construction. It consists of four main parts: ring gear, sun gear, planet gear and carrier gear. Since the three planet gears are connected to be a whole by the carrier gear, the planetary gear set can output three rotational shafts. Denoting the rotational speeds of ring gear, carrier gear and sun gear by ω_r, ω_c and ω_s, respectively, it yields:

$$w_s + kw_r - (k+1)w_c = 0 \qquad (\mathbf{1.4})$$

where *r s k = R R* , R_r and R_s are the radius of ring gear and sun gear, respectively.

Although mechanical gear works well in all kinds of applications, there is still much room for improvement. Since in mechanical gears, the movable parts are in mesh with each other through the metal teeth, these contact mechanisms can arouse many nuisances, such as, friction loss, audible noise, mechanical vibration and need of regular lubrication and maintenance. What is more, in the occasions of fluid controls, such as blood pumps and toxic gas pumps, mechanical gears are not able to offer satisfactory performance since they can not realize physical isolation between the input shaft and output shaft. For these reasons, the concept of non-contact torque transmission through the interaction of magnetic fields has attracted increasing

attention. Consequently, a magnet based non-contact gear is so-called the magnetic gear.

As well as mechanical gears, magnetic gears have different types as shown in Fig.1.24. When designing these types of magnetic gears, there are two rules that should be observed:

1. The pole numbers of PMs on each movable part should be even and the adjacent PMs should have opposite polarities.

2. The pole pitches of the PMs on the adjacent movable parts should be equal.

The first rule is to ensure the even distribution of magnetic fields. Generally, field flux should flow via closed loops that go through the adjacent PMs. For this reason, in what follows, *pole-pair numbers* is used to describe the quantity of the PMs that are involved in magnetic gears. The second rule is to ensure the good match of the adjacent movable parts. This can be understood by considering their mechanical analogues: In mechanical gears, the shapes of the teeth on the adjacent movable parts should be the same to make sure these parts can be well meshed. The speed variations in these types of magnetic gears are decided by the pole-pair numbers of PMs mounted on the adjacent movable parts. For example, for the spur gear given in Figure 1.24(a), the rotational speeds are governed by:

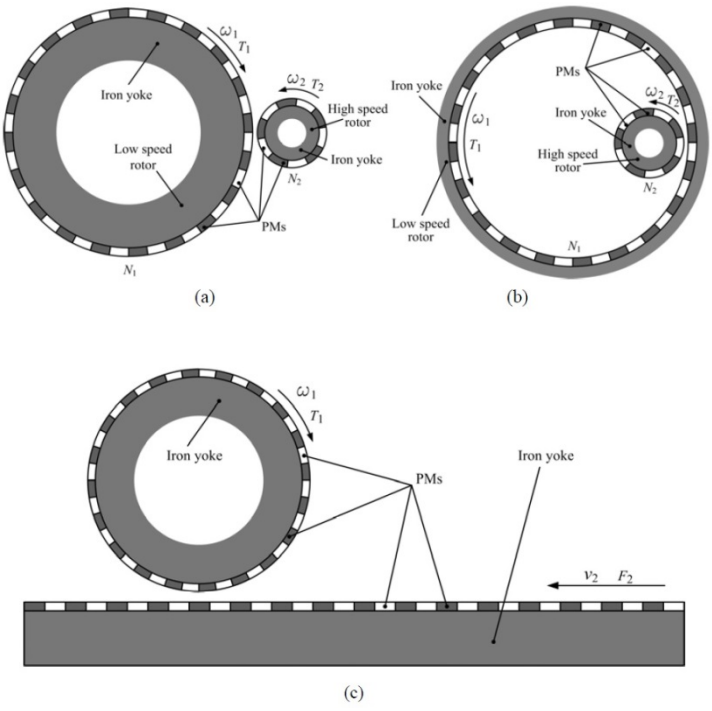

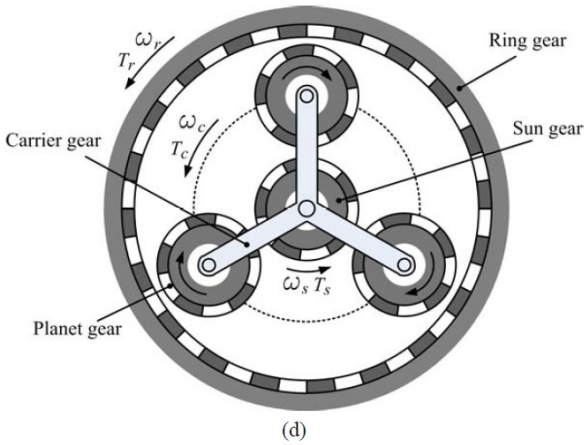

Figure 1.24: Early types of magnetic gears. (a) Spur gear. (b) Internal ring gear. (c)Rack and pinion. (d) Planetary gear [17].

$$\frac{w_1}{w_2} = -\frac{N_2}{N_1} \qquad (\mathbf{1.5})$$

where N_1 and N_2 denote the pole-pair numbers of the PMs mounted on the left-hand side rotor and right-hand side rotor, respectively.

These equations are basic mechanical equations. However, the most widespread and popular magnetic gear, that mentioned before, is coaxial magnetic gear. Coaxial magnetic gear has three rotational part, which contains inner rotor, middle stator (modulation ring) and outer rotor. Permanent magnets are mounted on inner rotor and outer rotor. In some application outer and inner rotor rotates and middle ring is stationary and also in some applications inner rotor and middle ring rotates and outer rotor is stationary [62-64]. Computation equations of pole pair numbers in magnetic gear and also gear ratio of coaxial magnetic gear will be explained with details in second chapter.

1.4 Tools of Analysis

Finite element analysis (FEA) has been used to simulate the behavior of the different magnetic gear variations. Maxwell by Ansoft, is used in this project. Maxwell uses the virtual work method of calculating torque for the moving bodies in its transient simulations. Ansoft maxwell, also, is one of powerful programs for 2D and 3D electromagnetic analysis. Using maxwell package we can compute Static electric fields, forces, torques, and capacitances caused by voltage distributions and charges, Static magnetic fields, forces, torques, and inductances caused by DC currents, static

external magnetic fields, and permanent magnets, Time-varying magnetic fields, forces, torques, and impedances caused by AC currents and oscillating external magnetic fields and Transient magnetic fields caused by electrical sources and permanent magnets. Rotational Machine Expert (RMxprt) is an interactive software package used for designing and analyzing electrical machines.

2. ANALYTICAL COMPUTATION OF MAGNETIC DISTRIBUTION FIELD AND MAGNETIC GEARING

2.1 Introduction

In this chapter the theory of magnetic gearing, the determination of the gear ratio and the calculation of the parameters of the equivalent circuit for a magnetically geared PM machine are presented. With the equivalent circuit parameters known the performance of the machine can be calculated. In the first section of this chapter magnetic gear theory will be described and in the second section permanent magnet generator theory.

2.2 The Operational Principles of Magnetic Gearing

Fundamental to the operation of a coaxial magnetic gear are the magnetic fields produced by the permanent magnets on either the high- or low-speed rotors by the steel pole pieces (flux-modulation pieces), which result in space harmonics having the same number of poles as the related magnet rotor. In Figure 2.1 a generic layout of a radial field magnetic gear is presented. The flux distribution in radial direction at a radial distance r and angle q produced by either permanent magnet rotor, without taking into consideration the flux-modulator, can be written in the following form [28,13]:

$$B_{rA} = \sum_{m=1,3,5,\dots} b_{rm}(r)\cos(mp(\theta - w_r t) + mp\theta_0) \qquad (\mathbf{2.1})$$

And the modulation function can be written as:

$$B_{rB}(r,\theta) = \lambda_{r0}(r) + \sum_{j=1,2,3,\dots} \lambda_{rj}(r)\cos\left(jn_s(\theta - w_s t)\right) \qquad (\mathbf{2.2})$$

The resultant field components for the radial component are:

$$B_r(r,\theta) = B_{rA}(r,\theta) \times B_{rB}(r,\theta) \qquad (\mathbf{2.3})$$

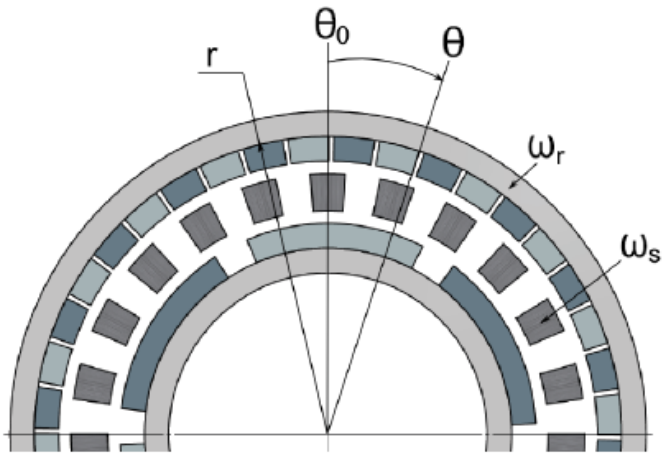

Figure 2.1: Magnetic gear parameters [28].

Similarly for the circumferential flux distribution, we have [28]:

$$B_{\theta A}(r,\theta) = \sum_{m=1,3,5,\ldots} b_{\theta m}(r)\sin(mp(\theta - w_r t) + mp\theta_0) \qquad (\mathbf{2.4})$$

$$B_{\theta B}(r,\theta) = \lambda_{r0}(r) + \sum_{j=1,2,3,\ldots} \lambda_{\theta j}(r)\, sin(jn_s(\theta - w_s t)) \qquad (\mathbf{2.5})$$

$$B_{\theta}(r,\theta) = B_{\theta A}(r,\theta) \times B_{\theta B}(r,\theta) \qquad (\mathbf{2.6})$$

where p is the number of pole-pairs on a permanent magnet rotor, ns is the number of modulation pieces, w_r is the rotational velocity of the permanent magnet rotor and w_s is the rotational velocity of the flux-modulator. The Fourier coefficients for the radial and circumferential flux density distribution without the flux-modulation pieces are; b_{rm} and $b_{\theta m}$, respectively. The Fourier coefficients for the radial and circumferential components of the flux density distribution resulting from the introduction of the flux-modulation pieces are λ_{rj} and $\lambda_{\theta j}$, respectively.

On substitution of 2.1 and 2.2, Eq.2.3 can be further expressed as:

$$\begin{aligned} B_r(r,\theta) = \lambda_{r0} & \sum_{m=1,3,5,\ldots} b_{rm}(r)\cos(mp(\theta - w_r t) + mp\theta_0) \\ & + \frac{1}{2}\sum_{m=1,3,5,\ldots}\sum_{j=1,2,3,\ldots} \lambda_{rj}(r) b_{rm}(r)\cos\left((mp + jn_s)\left(\theta - \frac{(mpw_r + jn_s w_s)}{mp + jn_s}t\right) + mp\theta_0\right) \\ & + \frac{1}{2}\sum_{m=1,3,5,\ldots}\sum_{j=1,2,3,\ldots} \lambda_{rj}(r) b_{rm}(r)\cos((mp - jn_s)\left(\theta - \frac{mpw_r - jn_s w_s}{mp - jn_s}t\right) \\ & + mp\theta_0) \end{aligned} \qquad (\mathbf{2.7})$$

Similarly on substitution of Equation 2.4 and 2.5, Equation 2.6 becomes:

$$B_\theta(r,\theta) = \lambda_{\theta 0} \sum_{m=1,3,5,\dots} b_{\theta m}(r)\, sin(mp(\theta - w_r t) + mp\theta_0) + \frac{1}{2} \sum_{m=1,3,5,\dots} \sum_{j=1,2,3,\dots} \lambda_{rj}(r) b_{rm}(r)\, sin\left((mp + jn_s)\left(\theta - \frac{(mpw_r + jn_s w_s)}{mp + jn_s} t\right) + mp\theta_0\right) + \frac{1}{2} \sum_{m=1,3,5,\dots} \sum_{j=1,2,3,\dots} \lambda_{rj}(r) b_{rm}(r)\, sin((mp - jn_s)\left(\theta - \frac{mpw_r - jn_s w_s}{mp - jn_s} t\right) + mp\theta_0) \quad (\mathbf{2.8})$$

From Equation 2.7 and 2.8, it can be seen that the number of pole pairs in the space harmonic flux density distribution produced by either the high- or low-speed rotor is given by:

$$p_{m,k} = |mp + kn_s|$$

$$m = 1,3,5, \dots \infty \quad (\mathbf{2.9})$$

$$k = 0, \pm 1, \pm 2, \pm 3, \dots \pm \infty$$

The rotational velocity of the flux density space harmonic is given by:

$$w_{m,k} = \frac{mp}{mp + kn_s} w_r + \frac{kn_s}{mp + kn_s} w_s \quad (2.10)$$

From Equation 2.10, it can be seen that the velocity of the space harmonics due to the introduction of the flux-modulator ($k \neq 0$), is different to the velocity of the rotor which carries the permanent magnets. Therefore, in order to transmit torque at a different speed (change the gear ratio), the number of pole pairs of the other permanent magnet rotor must be equal to the number of pole-pairs of a space harmonic for which $k \neq 0$. Since the combination m = 1 and k = -1 results in the highest asynchronous space harmonic, the number of pole-pairs of the other rotor must be equal to (n_s - p). In other words, In mechanical planetary gears, k is limited between -1 and 0. In magnetic gears, the highest torque transmission capability results when m=1 and k=-1, resulting in the relationship between the outer pole pairs p_L, inner pole pairs p_H, and stator pole pieces n_s, shown in (2.11).

$$p_L = |p_H - n_s| \rightarrow n_s = p_H + p_L \rightarrow p_H - n_s = -p_L \quad (\mathbf{2.11})$$

$$w_L = \frac{p_H}{p_H - n_s} w_H - \frac{n_s}{p_H - n_s} w_s \quad (\mathbf{2.12})$$

The gear ratio when the flux-modulator is held stationary (w_s = 0), is then given by;

$$G_r = \frac{p_H - n_s}{p_H} \qquad (\mathbf{2.13})$$

Or

$$G_r = -\frac{p_L}{p_H} \qquad (\mathbf{2.14})$$

which gives;

$$n_s = p_H + p_L \qquad (\mathbf{2.15})$$

where p_H and p_L are the number of pole-pairs on the high- and low-speed rotors, respectively. Sometimes, it may be preferred to keep the outer rotor stationary (w_r=0) as it may simplify the overall mechanical design. The torque will then be transmitted to the flux-modulator instead of the outer rotor, the gear ratio then becomes:

$$G_r = \frac{n_s}{p_H} \qquad (\mathbf{2.16})$$

2.3 Mechanical Torque and Power Calculation

In this section we will discuss about mechanical equations which help us in this project. As shown in Fig.2.2, a motor is used to drive a coaxial magnetic gear which is rotating a load. Thus, following equations are modeling figure below:

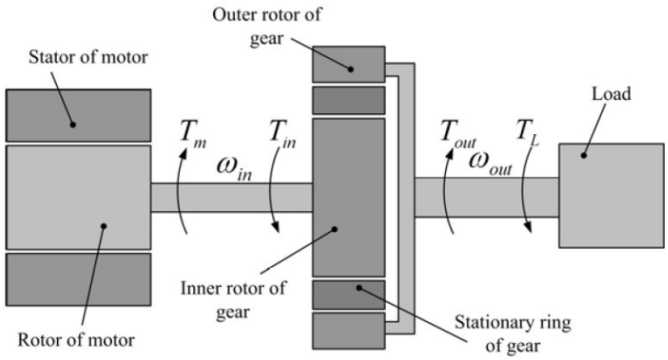

Figure 2.2: Torque coupling of motor and magnetic gear.

$$T_m = T_{in} + J_{in}\frac{dw_{in}}{dt} + B_{in}w_{in} \qquad (\mathbf{2.17})$$

$$T_{out} = T_L + J_{out}\frac{dw_{out}}{dt} + B_{out}w_{out} \qquad (\mathbf{2.18})$$

Where J_{out} and J_{in} are moment of inertia of inner and outer rotors and B_{in} and B_{out} are damping factors. It is obvious that unit of angular velocity (w) is rad/sec.

The following equation is used to convert unit of w from rpm (rev-per-minute or min^{-1}) to rad/s

$$w_{rad/s} = \frac{2\pi w_{rpm}}{60} \qquad (\mathbf{2.19})$$

Eq.2.20 is used to calculate power in mechanical systems:

$$P = T.w_{rad/s} \qquad (\mathbf{2.20})$$

2.4 The Equivalent Circuit of a Magnetically Geared Permanent Magnet Generator (MGPMG)

2.4.1 Magnetically decoupled MGPMG

For a magnetically decoupled MGPMG the per phase electrical equivalent circuit of the PMG is shown in Figure 2.2(a). In this circuit, E_1 is the electromotive force (EMF) induced in the stator windings due to the fundamental air-gap PM flux-linkages of the high-speed rotor, L_s is the stator inductance, R_s is the stator resistance and I_s is the stator current. The shunt resistance R_c is the core loss resistance. With the 2-D finite element method the total stator flux-linkage can be calculated, however the end winding flux-linkage is not calculated in 2-D FEM. Thus the stator inductance L_s is split into two terms, namely the main inductance L_m and the end winding leakage inductance L_e, as shown in Figure 2.2 (b). In the circuit R_c may be shifted to the left of L_e as an approximation. The approximation allows that the left side of the equivalent circuit marked by the dashed lines can be accurately calculated by directly using finite element method.

In this section the rest of the electrical parameters that are not accounted for in the FEM analysis will be calculated. The following equations and performance calculation approach is inspired from [47;70]. Thus, all of the parameters on the right side of Figure 2.2 (b) will be calculated. The corresponding steady state *d* and *q*-axis equivalent circuits are shown in Figure 2.3.

The flux-linkages λ_d and λ_q are the *d*- and *q*-axis stator flux-linkage (λ_{dq0}) components.

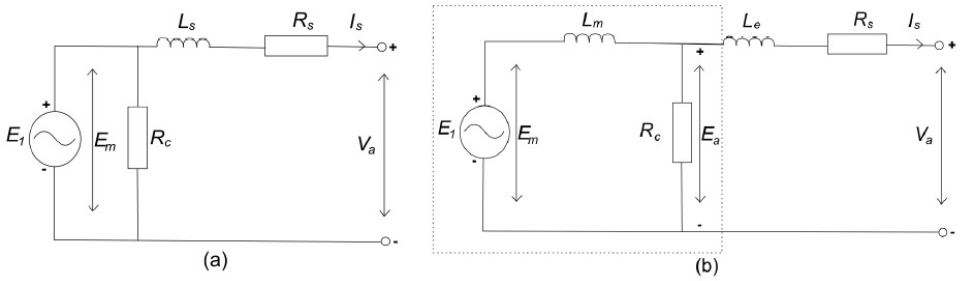

Figure 2.3: Per phase equivalent circuits [47].

Park's transformation K_p is used to transform the equivalent circuit in the *abc* reference frame to the equivalent circuits in the d_q reference frame:

$$K_p = {}^{2}/_{3}\begin{bmatrix} \cos\theta & \cos(\theta - 2\pi/3) & \cos(\theta + 2\pi/3) \\ \sin\theta & \sin(\theta - 2\pi/3) & \sin(\theta + 2\pi/3) \\ 1/2 & 1/2 & 1/2 \end{bmatrix} \qquad (\mathbf{2.21})$$

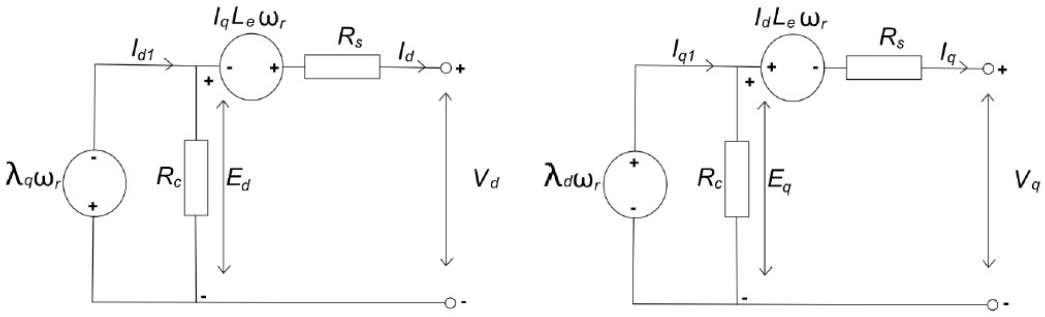

Figure 2.4: Decoupled *dq* equivalent circuits [70].

As mentioned, the input of the equivalent circuit are the parameters calculated in the FE analysis, however the input of the FE analysis are the instantaneous three phase currents i_{abc}. The instantaneous three phase currents can be calculated by determining the maximum allowable current-density that the given stator coils can handle. Thus, the amplitude of the current space phasor *I* can be calculated from the input current density *J* with the following formula

$$I = \sqrt{2} J A_{cu} n_a / z \qquad (\mathbf{2.22})$$

where A_{cu} is the available area for placing conductors (copper) in mm^2, n_a is the number of parallel circuits and z is the number of turns per coil. Equation 2.19 can be used to calculate the available conductor area A_{cu}.

$$A_{cu} = A_c * k_f \quad (\mathbf{2.23})$$

where A_c is the coil cross-section area and k_f is the filling factor, which is calculated with the following equation

$$k_f = A_{con} z n_{strands} / A_c \quad (\mathbf{2.24})$$

In the equation A_{con} is the area of a single conductor and $n_{strands}$ is the number of strands per conductor. The instantaneous three-phase currents can then be calculated and used as inputs to the FE analysis and the three phase flux-linkages λ_{abc} will be the output of the FE analysis. With the three phase flux-linkages and Park's transformation the d_q flux-linkages λ_{dq0} can be determined

$$[\lambda_{dq0}] = [K_p][\lambda_{abc}] \quad (\mathbf{2.25})$$

From this the speed voltages E_d and E_q of the equivalent circuit can be determined.

$$E_d = -\lambda_q w_r \quad E_q = \lambda_d w_r \quad (\mathbf{2.26})$$

Next the core-loss resistance R_c needs to be calculated, R_c is calculated with the RMS value of the phase EMF, E_a, and the total core losses P_c. The RMS value of the phase EMF, E_a, is calculated with the following equation

$$E_a = \sqrt{\frac{E_d^2 + E_q^2}{2}} \quad (\mathbf{2.27})$$

and the total core losses P_c are determined in the FEM analysis. Thus, R_c is calculated with the following equation:

$$R_c = \frac{3E_a^2}{P_c} \quad (\mathbf{2.28})$$

The next step is to calculate the d_q currents i_{dq0}. The dq currents can be calculated with Park's transformation and the instantaneous three phase currents i_{abc} as determined in Equation

$$[i_{dq0}] = [K_p][i_{abc}] \quad (\mathbf{2.29})$$

From the known d_q current components (I_d and I_q), the calculated d_q speed voltages (E_d and E_q) and the core loss resistance R_c, the d_{q1} current components (I_{d1} and I_{q1}) and the current amplitude I_{s1} can be calculated:

$$I_{d1} = I_d + E_d/R_c$$

$$I_{q1} = I_q + E_q/R_c \quad (\mathbf{2.30})$$

$$I_{s1} = \sqrt{I_{d1}^2 + I_{q1}^2}$$

Next the end-winding inductance per phase is calculated with [71];

$$L_e = \frac{4\mu_0 n_{tp}^2 l_e P_{le}}{p q_1} \quad (\mathbf{2.31})$$

where μ_0 is the permeability of air (μ_0=4π10^{-7}), n_{tp} is the number of turns in series per phase, q_1 is the number of coils per pole per phase and l_e is the end-winding length of a coil. Then the d_q inductances are determined from the following equations:

$$L_q = \lambda_q/I_q \quad (\mathbf{2.32})$$

And

$$L_d = L_q \quad (\mathbf{2.33})$$

After this the per phase stator winding resistance can be calculated [70],

$$R_s = \frac{2n_{tp}(l + l_e)}{\sigma_T n_a s_{cu}} \quad (\mathbf{2.34})$$

Where l is the active length of a coil, S_T is the electric conductivity of the wire at temperature T and s_{cu} is the cross section area of the wire. The skin effect has not been taken into account in Equation 2.30. The skin effect is minimal if thin parallel wires are used. With the per phase stator winding resistance (Rs) and the current amplitude (I_{s1}), the total copper losses can be determined:

$$P_{cu} = 3I_{s1}^2 R_s \quad (\mathbf{2.35})$$

The d_q terminal voltage components (V_d and V_q) and the voltage amplitude are calculated from:

$$V_d = E_d + L_e I_q w_r - I_d R_s \quad (\mathbf{2.36})$$

$$V_q = E_q + L_e I_d w_r - I_q R_s \quad (\mathbf{2.37})$$

$$V_s = \sqrt{V_d^2 + V_q^2} \tag{2.38}$$

Steady state torque T_{He} of the high-speed rotor can also be calculated from the equivalent circuit elements, by:

$$T_{He} = \frac{3}{2} P\left(\lambda_d I_q - \lambda_q I_d\right) \tag{2.39}$$

With the gear ratio Gr of the magnetic gear known, the steady state torque of high-speed rotor referred to low-speed side can be calculated as:

$$T_{Le} = T_{He} \times G_r \tag{2.40}$$

The next step is to calculate the apparent power S:

$$S = \frac{3}{3} V_s I_s \tag{2.41}$$

Then the power factor is determined from the following equation:

$$P_f = \cos(\tan^{-1}(\frac{V_d}{V_q}) \pm \tan^{-1}(\frac{I_d}{I_q})) \tag{2.42}$$

With the apparent power S and the power factor P_f the output power P_{out} is calculated:

$$P_{out} = SP_f \tag{2.43}$$

The input power of MGAFG P_{in} is calculated from the output power and the total losses P_{Loss}:

$$P_{in} = P_{out} + P_{loss} \tag{2.44}$$

where P_{Loss} consists of; the copper losses P_{cu}, the core losses P_c, the losses of the magnetic gear part of the machine P_{gear} and the windage losses $P_{windage}$.

$$P_{loss} = P_{cu} + P_c + P_{gear} + P_{windage} \tag{2.45}$$

And finally the efficiency η can be calculated:

$$\eta = \frac{P_{out}}{P_{in}} \tag{2.46}$$

Thus, the machine performance can be accurately calculated by simulating the machine in a FE analysis, extracting the results and further processing the machine parameters with the help of the equivalent circuit.

2.4.2 Magnetically coupled MGPMG

For the coupled system the flux-linkage of the low-speed rotor contribute to the total flux-linkage in the stator. Thus a secondary EMF source E_2 is introduced in the equivalent circuit (see Figure 2.4). The speed voltage components of Equation 2.22 will thus have another flux-linkage component due to the flux-linkage contribution of the low-speed rotor. Thus the total d_q flux-linkages becomes:

$$\lambda_d = \lambda_{dH} + \lambda_{dL} \qquad \lambda_q = \lambda_{qH} + \lambda_{qL} \tag{2.47}$$

where the subscripts H and L are the high- and low-speed rotor contributions, respectively. Even though the high- and low-speed rotors rotate at different velocities, the rotational velocity w_r of the high-speed rotor is still used in Equation 2.22 to calculate the speed voltages, since the flux-modulator modulates the flux component of the low-speed rotor at the same velocity as that of the high-speed rotor's flux component.

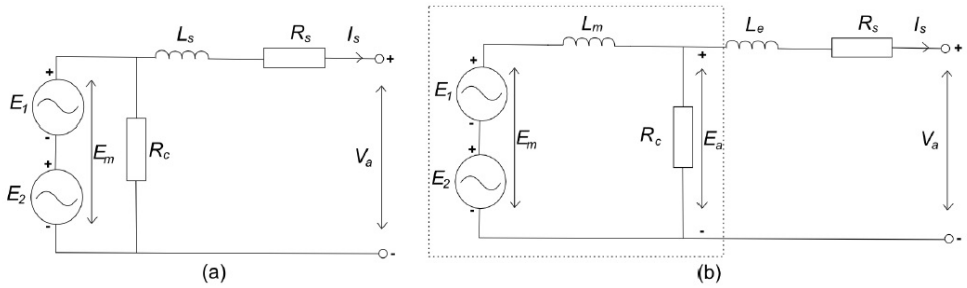

Figure 2.5: Coupled per phase equivalent circuits [70].

3. DESIGN TECHNICS AND SIMULATION RESULTS

In this project new configuration of coaxial magnetic gear which has improved capability is presented. As mentioned before, coaxial MG is used frequently in industry because of higher efficiency. As an example spur type magnetic gear is one of first generation of magnetic gears and as result of its structure, effective flux restricted and this causes a reduced efficiency. However, flux which is produced in coaxial magnetic gear is used completely and it is not wasted, also all magnets are involved in creating torque, hence efficiency is higher. One of famous coaxial magnetic gears is called surface mounted magnetic gear (Fig.3.1).

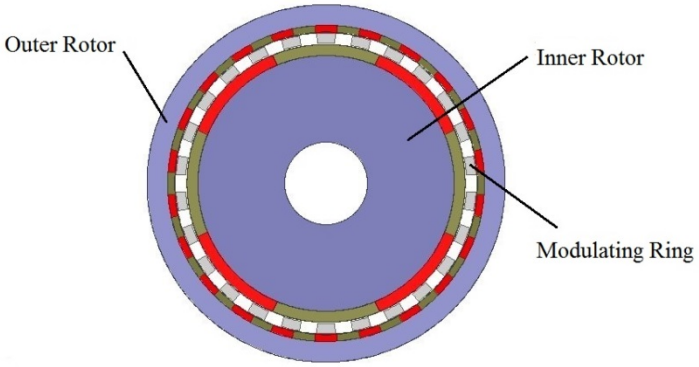

Figure 3.1: Surface mounted magnetic gear.

3.1 Conventional Magnetic Gearing Structure and Analysis

Figure 3.1 is an ordinary conventional coaxial MG which its dimensions are chosen from reference [59] (see Table 3.1). Using Ansoft Maxwell, we applied static analyses and steady state analyses. Static analysis is an analysis which one side is steady and the other side rotates with constant speed. Steady state analysis is an analysis which two rotor rotate with constant speed satisfying gear ratio.

During analyses we consider some conditions. For example, we assume middle ring, which is named modulating ring or stator pole pieces, stationary. Hence using Eq.2.14 gear ratio is equal to 5.5.

$$G_r = \frac{22}{4} = 5.5 \qquad (\mathbf{3.1})$$

Thus when inner rotor rotates with 330 min^{-1} outer rotor rotates with 60 min^{-1}.

Table 3.1: Dimension of coaxial surface mounted magnetic gear [59].

Parameters	Value
Inner radius of inner rotor	30 mm
Outer radius of inner rotor	101 mm
Outer radius of inner rotor yoke	93 mm
Magnetic thickness of inner rotor	8 mm
Inner pole pair	4
Inner radius of outer rotor	110 mm
Outer radius of outer rotor	130 mm
Inner radius of outer rotor yoke	115 mm
Magnet thickness of outer rotor	5 mm
Outer pole pairs	22
Inner radius of stator pole pieces	102 mm
Outer radius of stator pole pieces	109 mm
Stack length	50 mm

As result of pole pair numbers our magnetic gear has 180 degrees symmetry, so that we can divide it to two in order to reduce analysis time (Fig.3.2). Furthermore, Fig.3.3 shows the mesh segments which should be applied in FE softwares to analyze our gear accurately. All analyses and results shown in this thesis are done by means of Ansys Maxwell.

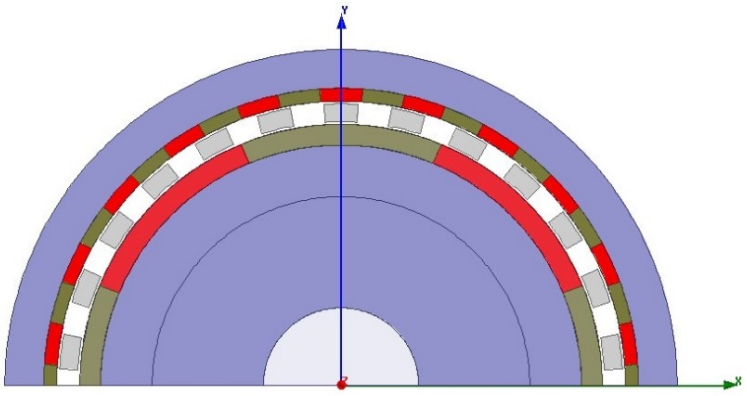

Figure 3.2: 180 degrees symmetry.

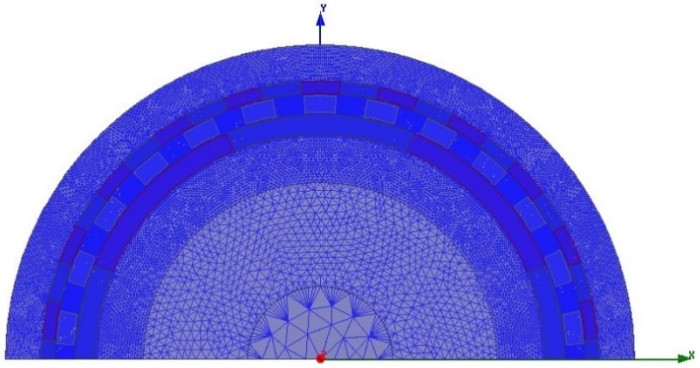

Figure 3.3: Mesh applying on symmetry model.

3.1.1 Conventional magnetic gear using neodymium

Among famous permanent magnets, NdFeB (Neodymium) is the strongest rare-earth magnet which is known till now. Neodymium Also known as Neo, these are the strongest and most controversial magnets. They are in the rare earth family because of the Neodymium (Nd), Boron (B), Dysprosium (Dy), Gallium (Ga) elements in their composition. A relatively new group of commercial magnets, they are controversial because they are the only magnets that have been patented for both composition and processing.

The torque diagrams in static analysis and steady state analysis are shown in Fig.3.4 and Fig.3.5. As it mentioned in pervious section, dimensions are chosen from reference [59], hence, the result shown in Fig 3.4 is the same as the result of reference [59]. In all static analysis we assume outer rotor's speed 60 min^{-1} and inner rotor's speed zero and in steady state analysis we consider inner rotor rotate at 330 min^{-1} and outer rotor's speed at 60 min^{-1}.

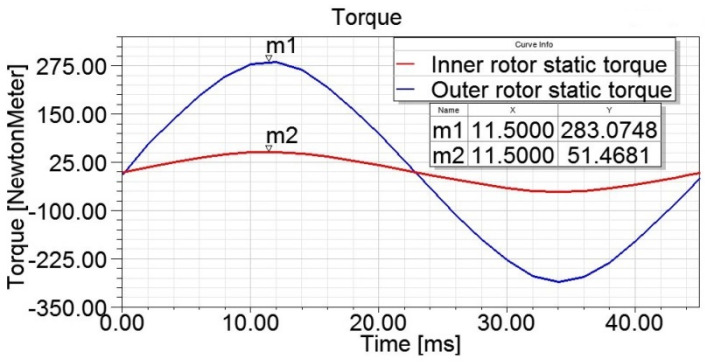

Figure 3.4: Static analysis of the surface mounted MG using Neodymium.

As it is seen here in Fig.3.4 maximum torque of outer rotor is 283 N.m and inner rotor is 51.46 N.m . Maximum torque which is being obtained implies maximum load that a rotor can handle it.

Consequently, maximum value of outer torque over maximum value of inner torque is equal to gear ratio which is 5.5. In steady state analysis two constant torques, each with constant value and little ripple can be generated (see Figure 3.5), also, gear ratio is obviously equal to 5.5.

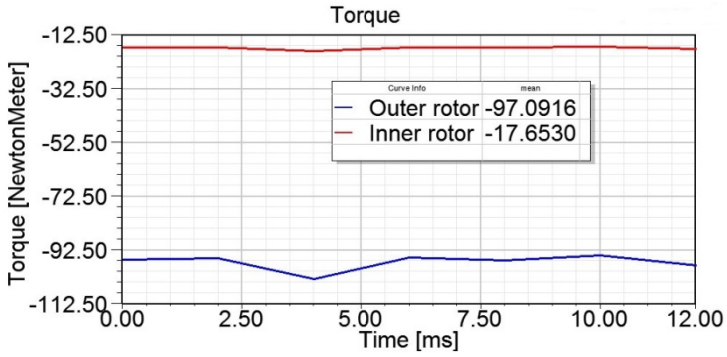

Figure 3.5: Steady state analysis of the surface mounted MG using Neodymium.

Please note that according to Eq.2.12 and 2.14, inner rotor and outer rotor rotate at opposite direction. Moreover, when outer rotor is constant, middle ring and inner rotor rotate at same direction.

3.1.2 Conventional magnetic gear using SmCo and Alnico

After NdFeB, Samarium Cobalt is second strongest magnet type. They belong to the rare earth family because of the Sm and Co elements in their composition. Magnetic properties are high and they have very good temperature characteristics. They are also more expensive than the other magnet materials. They come mostly in two grades: SmCo5 and Sm2Co17, also known as SmCo 1:5 and 2:17. Common uses are in aerospace, military and medical industries.

Alnico is one of the oldest commercially available magnets and have been developed from earlier versions of magnetic steels. Primary composition is Aluminum (Al), Nickel (Ni) and Cobalt (Co), hence the name. Although they have a high remnant induction, they have relatively low magnetic values because of their easy of demagnetization. However, they are resistant to heat and have good mechanical

features. Common applications are in measuring instruments and high temperature processes such as holding devices in heat treat furnaces.

Using same conditions, static and steady state analyses have been done on surface mounted magnetic gear, however, material type of magnets has been changed.

Figure 3.6 is static analysis of conventional magnetic gear using SmCo. In this figure peak value is lower than figure 3.4, because SmCo is not as strong as NdFeB and flux density is decreased. Figure 3.7 describes steady state analysis of MG, that inner rotor has a constant torque with small ripple. Please note that ripple in outer rotor torque is much lower than inner rotor. The reason is that inner rotor is smaller in size and lighter in weight than outer rotor.

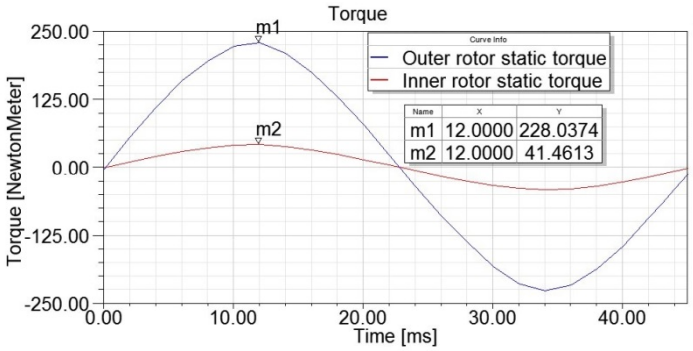

Figure 3.6: Static analysis of MG using SmCo.

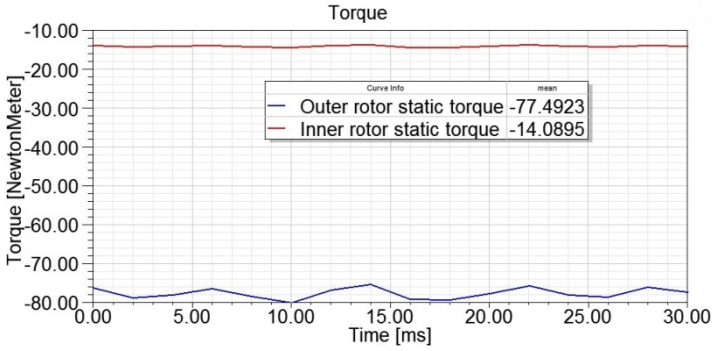

Figure 3.7: Steady state analysis of MG using SmCo.

Figure 3.8 is static analysis of MG using Alnico which obviously shows that alnico is much weaker than other magnet types. Moreover, inner and outer rotors have much greater ripple in steady state analysis (Fig.3.9). As a result of weakness of alnico, ripple is more sensible than Fig.3.5 and Fig.3.7. As it was mentioned before ripple of inner torque is more than outer torque. Please note that peak values of static analysis and mean values of steady state analysis should satisfy the gear ratio.

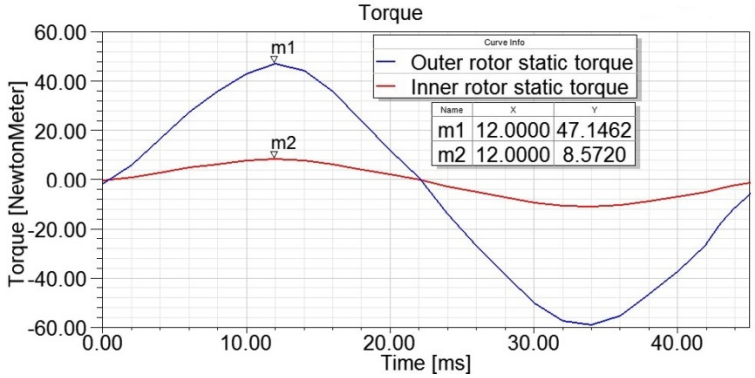

Figure 3.8: Static analysis of magnetic gear using Alnico.

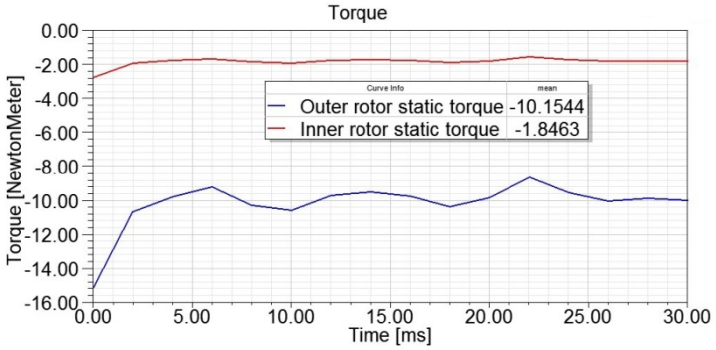

Figure 3.9: Steady state analysis of magnetic gear using Alnico.

3.1.3 Comparison of magnets and conclusion

As a conclusion, in Table 3.2 comparison of magnetic gears with different types of magnets is presented. The values which are shown in Table 3.2 has been presented in pervious figures.

Table 3.2: Comparison of magnetic gear using different magnet types

Magnetic gears	Steady state analysis at 330/60 min^{-1}	Static analysis outer rotor rotates at 60 min^{-1}
Surface mounted MG using NdFeB	97.09/17.6 N.m	283.07/51.46 N.m
Surface mounted MG using SmCo	77.49/14.08 N.m	228.03/41.46 N.m
Surface mounted MG using Alnico	10.15/1.86 N.m	47.14/8.5 N.m

From pervious section it is clear that alnico is the weakest rare-earth magnet and NdFeB is the strongest one. After some research about price of magnets in world

market, we can figure out that Alnico price is 20 $/Kg , price of SmCo is 70$/Kg and price of NdFeB 35 $/Kg (Table 3.3).

Table 3.3: Comparison of magnets relative cost.

Type	BH_{max}	$/kg	$/$BH_{max}$
Alnico 9	5	20 $	4 $
SmCo	25	70 $	2.8 $
NdFeB	40	35 $	0.88 $

SmCo is the expensive magnet type and not as strong as NdFeB, thus according to information in Table 3.3 NdFeB is the most economical type of magnets. Hence it is better to use Neodymium in magnetic gear because it is strong and price is economical.

3.2 Proposed Configuration of Magnetic Gear

According to pervious results, we started to think about second idea which was changing structure of gear. The first structure was spoke type magnetic gear (Fig.3.10).

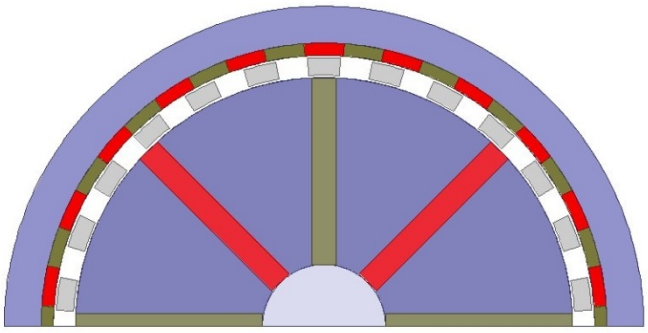

Figure 3.10: Spoke type MG with the same dimension as surface mounted

In Fig.3.10 all dimensions are the same as conventional magnetic gear. In order to compare spoke type MG with conventional MG we set static analysis too. The result of static analysis is shown in Fig.3.12. As you can see, peak value of static torque is diminished. One of reasons that causes' decreasing the torque is that for about 1/3 of magnet which is near the shaft is useless. The flux generated in that part wastes due to closed flux path which is involved in one magnet only (see Fig.3.11).

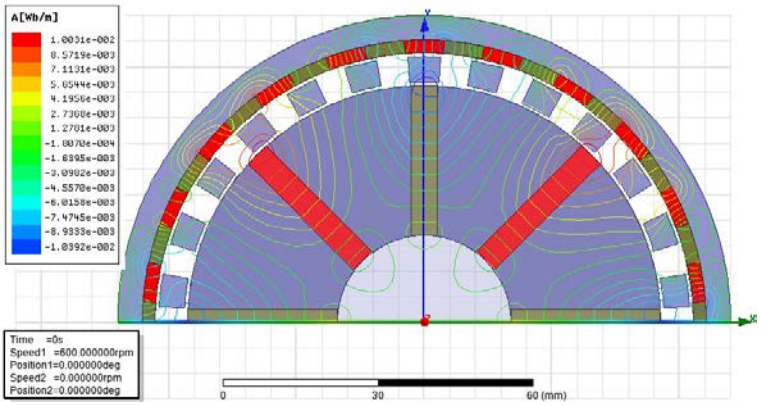

Figure 3.11: Flux lines of the spoke type MG.

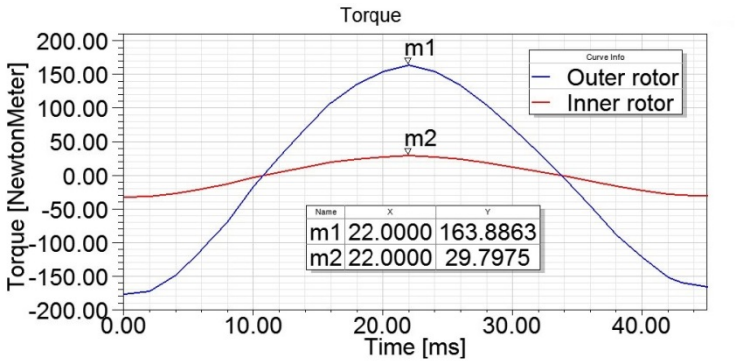

Figure 3.12: Torque diagram of the spoke type MG.

This structure has two problems. First, torque rate is not competitive with surface mounted MG in same rang of dimensions. Second, this idea is not innovative. Hence, using IPM type rotor for inner rotor was next idea.

Figure 3.13 shows IPM type rotor permanent magnet magnetic gear. In this structure there are some important factors which need to be explained. First of all, outer rotor is the same as rotor which in used in conventional type, dimension of inner rotor magnets are the same as magnets which is used in conventional form and detail of inner rotor dimension is given in Table 3.4. It is better to imagine that length of V form magnets is the same as length of curved magnets in surface mounted magnetic gear.

In this new structure the empty part between two magnets near the surface will be filled with non-magnetic material such as aluminum. The reason that we used this aluminum is to keep the magnets tight and steady during rotation. Rotor cores are laminated so that we assumed those holes on each layer in order to lock them up via those holes. Material used for cores is non-oriented steel named M-36.

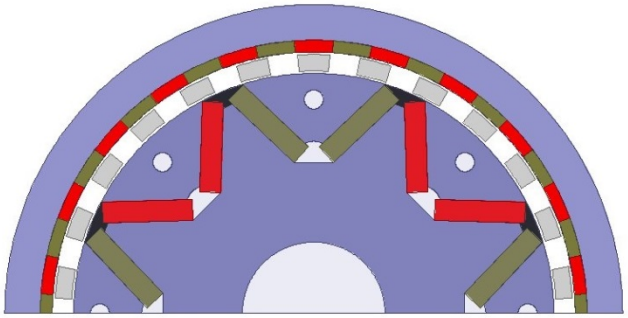

Figure 3.13: IPM type rotor permanent magnet magnetic gear.

Table 3.4: Dimension of the proposed magnetic gear [59].

Parameters	Value
Inner radius of inner rotor	30 mm
Outer radius of inner rotor	101 mm
Radius of little holes in inner rotor	4 mm
Magnetic thickness of inner rotor	8 mm
Width of V form magnets	76 mm
Inner pole pair	4
Inner radius of outer rotor	110 mm
Outer radius of outer rotor	130 mm
Inner radius of outer rotor yoke	115 mm
Magnet thickness of outer rotor	5 mm
Outer pole pairs	22
Inner radius of stator pole pieces	102 mm
Outer radius of stator pole pieces	109 mm
Stack length	50 mm

M-36 is kind of laminated silicon steel. Addition of 0.5% to 3.25% of silicon (Si) increases the resistivity (reduces eddy current losses) and improves magnetization curves B–H of low carbon steels. Silicon content , however, increases hardness of laminations and, as a consequence, shortens the life of stamping tooling. Non-oriented electrical steels are Fe-Si alloys with random orientation of crystal cubes and practically the same properties in any direction in the plane of the sheet or ribbon. Non-oriented electrical steels are available as both fully processed and semi-processed products. Fully processed steels are annealed to optimum properties by manufacturer and ready for use without any additional processing. Semi-processed steels always require annealing after stamping to remove excess carbon and relieve stress. Better grades of silicon steel are always supplied fully processed; while semi processed silicon steel is available only in grades M43 and worse. In some cases, users prefer to develop the final magnetic quality and achieve relief of fabricating

stresses in laminations or assembled cores for small machines. In this project we used M-36, because according to datasheet this material has better B-H curve.

Now we set static analysis and steady state analysis for obtaining torque diagram so that we can compare diagrams with conventional form. Fig.3.14 and Fig.3.15 are describing static and steady state analyses respectively.

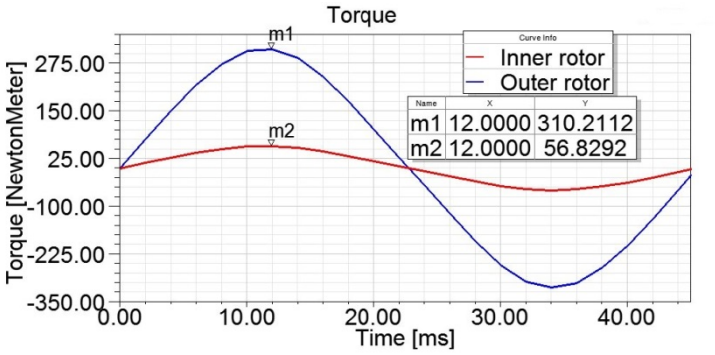

Figure 3.14: Static analysis of the proposed magnetic gear.

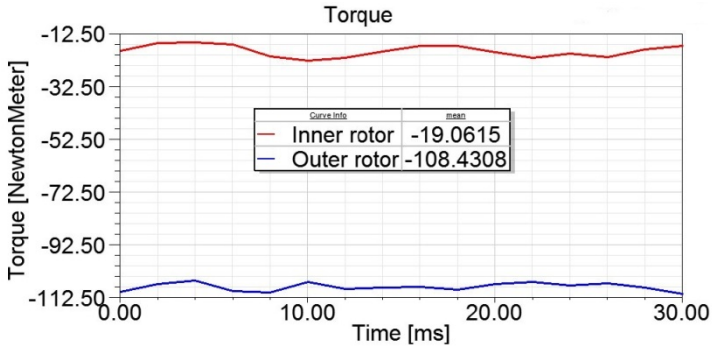

Figure 3.15: Steady state of the proposed magnetic gear.

A little comparison will show that the peak value of the torque in static analysis and mean value of the constant torque in steady state analysis is much greater that conventional form. In conventional form peak value of static torque of outer rotor is equal to 283.07 N.m, however in proposed structure peak value of static torque of outer rotor is equal to 310.21 N.m which shows that we have had 9.5 percent growth in torque. This maximum torque shows that our rotor can handle greater load. Fig.3.16 shows mesh plot which we applied for analysis, moreover, Fig.3.17 shows flux lines and magnetic field distribution on magnetic gear at the same picture.

As it was mentioned before, we had 9.5% improvement in torque. In next sections transient analyses and efficiency computation for the magnetic gear will be

discussed. Table 3.5, which is given as a conclusion of this section, shows that the proposed magnetic gear has higher torque capability.

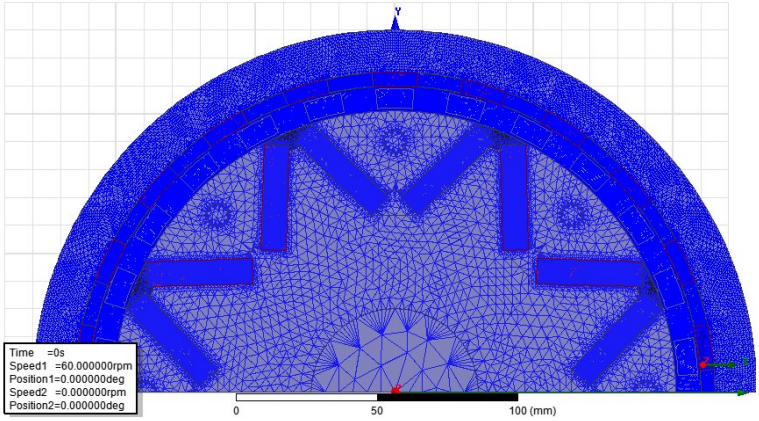

Figure 3.16: Mesh applied on magnetic gear.

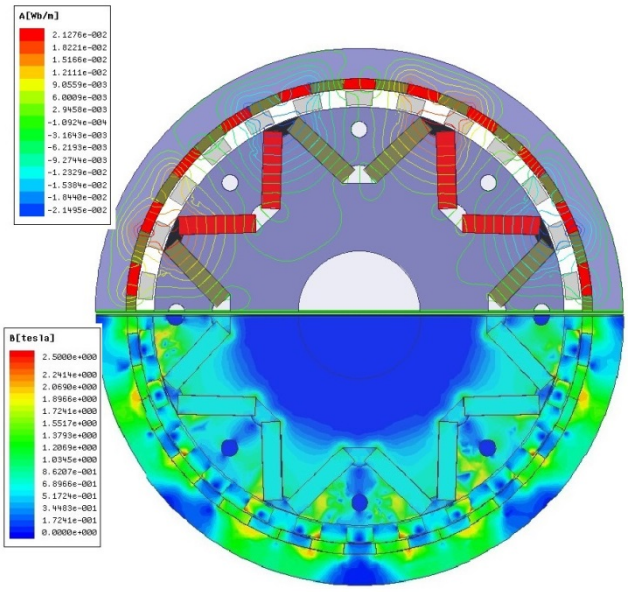

Figure 3.17: Magnetic field distribution and flux lines.

Table 3.5: Comparison of different types of MG with the proposed MG

Magnetic gears	Static analysis outer rotor rotates at 60 min^{-1}
Surface mounted MG	283.07/51.46 N.m
Spoke type MG	163.88/29.79 N.m
Proposed MG	310.21/56.82 N.m

3.3 Transient Analysis of Proposed Magnetic Gear

As it was explained previously, static analysis is an analysis that we assume one rotor steady and the other rotating at constant speed. Moreover, in steady state analysis we assume that inner rotor and outer rotor rotate at constant speed which satisfies gear ratio.

However, in transient analysis we consider some mechanical conditions. One of rotors, which in this project is inner rotor, is assumed as input and the other rotor that in this project is outer rotor, is assumed as output. For inner rotor we set a constant speed, as an illustration, consider a motor that is connected to input of gear and rotates the inner rotor with constant speed which is equal to 330 min^{-1}.

In transient analysis, despite of steady state analysis that outer rotor rotates at constant speed, we set outer rotor rotates freely in order to see outer rotor's response at different loads. Hence, in transient analysis we have some additional mechanical settings. According to Eq.2.18 we have 3 mechanical factors for outer rotor ration which is important. First moment of inertia (J_{out}), damping (B_{out}) and load torque (T_L). First of all we will present computation of moment of inertia for outer rotor which is cylindrical shape:

$$J_{out} = \frac{1}{2} m_{out}(R_1^2 + R_2^2) \qquad (\mathbf{3.2})$$

Where m_{out} is mass of outer rotor including magnets and core and dimension is kg, R_1 and R_2 are inner radius and outer radius of outer rotor respectively that dimension is m^2.

Equation bellow is used for calculation of outer rotor mass.

$$m_{out} = vd \qquad (\mathbf{3.3})$$

Where v is volume of rotor that dimension is cm^2 and d is density that is equal to 7.5 g/cm^2. Consequently, using Eq.3.2 and Eq.3.3 and substitution corresponding values of parameters, m_{out} and J_{out} can be computed as following:

$$m_{out} = \left(\pi \times 5(13^2 - 11^2)\right) \times 7.5 = 5654.87\ g\ \approx 5.6\ kg$$

$$J_{out} = \frac{1}{2} 5.6(0.11^2 + 0.13^2) = 0.0812\ \ kg.m^2$$

After computation of inertia we will apply some analyses including different loads. We anticipate seeing some facts. Speed of inner rotor in constant and outer rotor rotates freely, hence we expect that outer rotor, which oscillates for a while, settles at speed that satisfies gear ratio. In other words, according to Eq.2.14 when inner rotor which is high speed rotor rotates at 330 min^{-1}, outer rotor (low speed rotor) should rotates at -60 min^{-1}. The minus sign illustrates direction of outer rotor which is in opposite direction of inner rotor direction. Second fact that we expect to see is that, when our system reaches to steady state torque should follow the gear ratio. Third fact also, is that outer rotor torque should satisfy Eq.2.18 in steady state condition.

And the last fact, says that if load is greater than gear capability torque cannot follow the gear ratio.

In first analysis we chose no load condition. Thus, T_L=0, J_{out}=0.0821 and B_{out}=0.3. Please pay attention that damping is a mechanical factor and depends on kind of load, shaft of rotor, environmental conditions and etc. Hence, we assume damping small. Now Fig.3.18 and Fig.3.19 present torque and speed diagram of transient analysis in no load condition respectively.

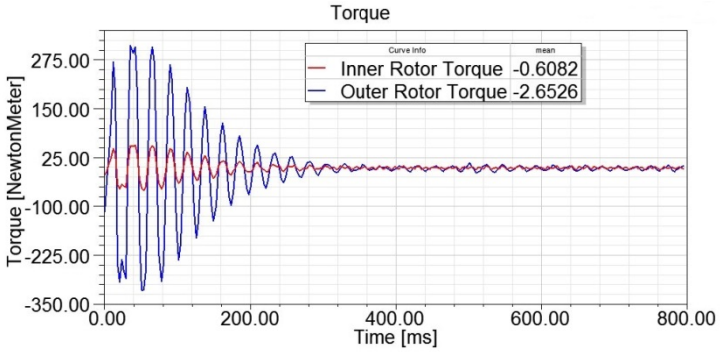

Figure 3.18: Torque diagram of transient analysis in no-load condition.

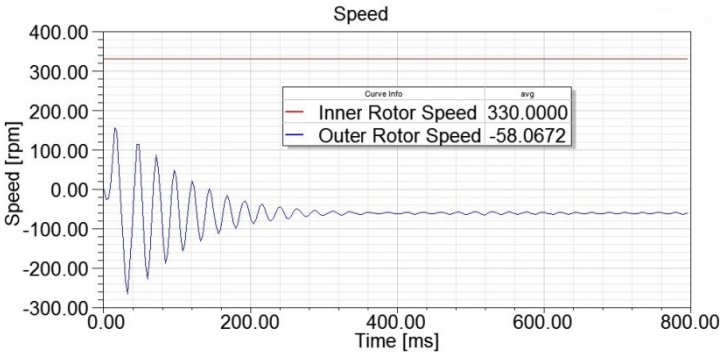

Figure 3.19: Speed diagram of transient analysis in no-load condition.

Figure 3.20 and 3.21 are torque and speed diagram of transient analysis with assuming of T_L=100 N.m respectively. Moreover, Fig.3.22 is related to torque diagram and Fig.3.23 is related to speed diagram when load is equal to 200 N.m .

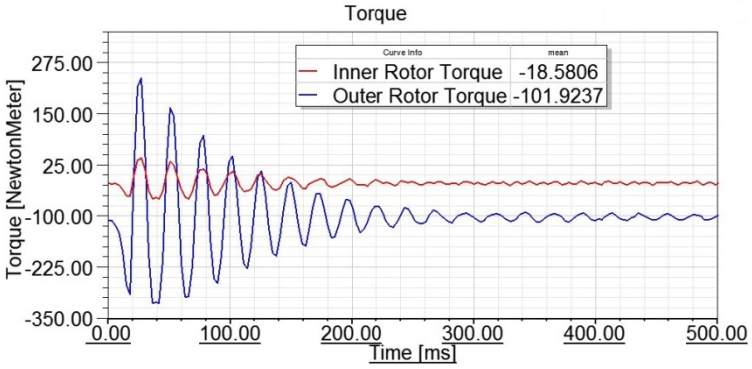

Figure 3.20: Torque diagram of transient analysis when load is equal to 100 N.m .

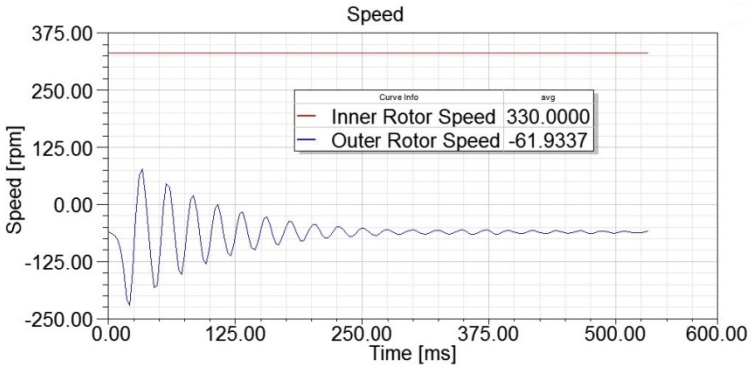

Figure 3.21: Speed diagram of transient analysis when load is equal to 100 N.m .

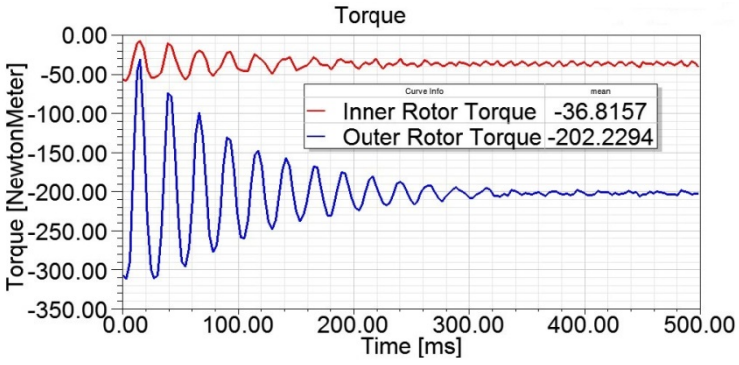

Figure 3.22: Torque diagram of transient analysis when load is equal to 200 N.m .

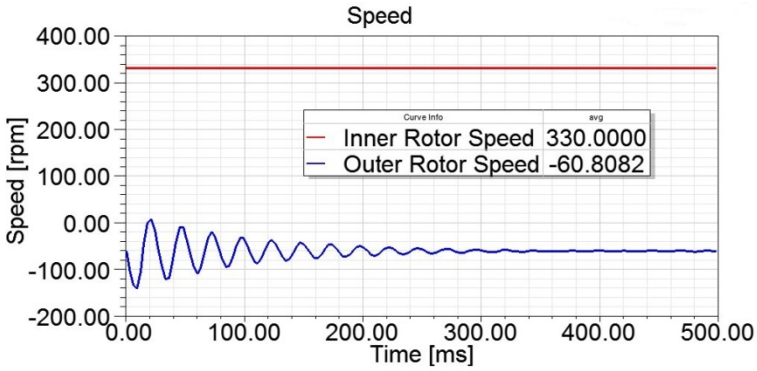

Figure 3.23: Speed diagram of transient analysis when load is equal to 200 N.m .

Figure 3.24 and figure 3.25 are related to torque and speed diagram of magnetic gear respectively when load is equal to 300 N.m , but we must pay attention that maximum torque that proposed gear can handle is 310 N.m according to static analysis. Consequently, torque may have a little oscillation.

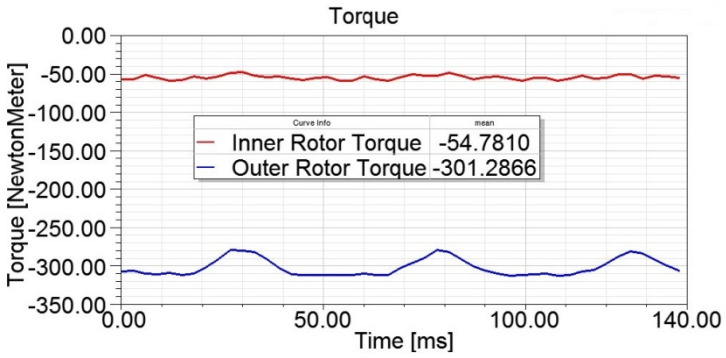

Figure 3.24: Torque diagram of transient analysis when load is equal to 300 N.m .

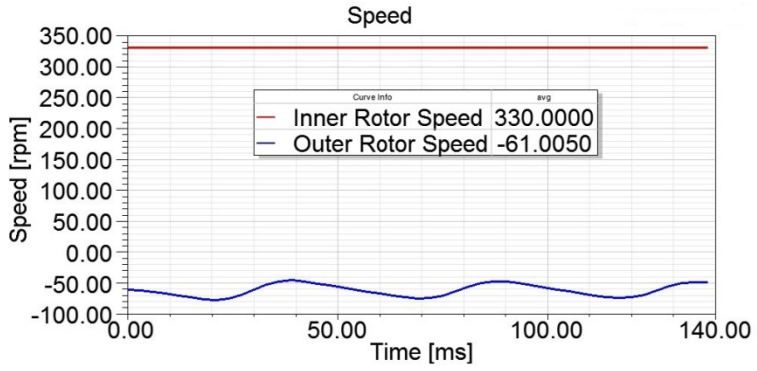

Figure 3.25: Speed diagram of transient analysis when load is equal to 300 N.m .

Now in order to prove forth fact we applied an analysis in load equal to 350 which is more than the maximum torque that gear can handle (see Figure 3.26 and 3.27).

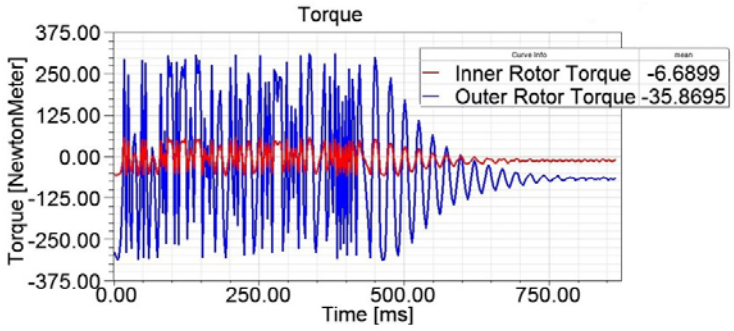

Figure 3.26: Torque diagram of transient analysis when load is equal to 350 N.m .

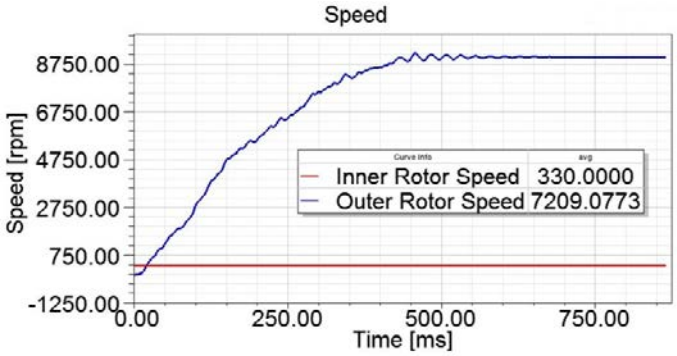

Figure 3.27: Speed diagram of transient analysis when load is equal to 350 N.m .

In figure 3.26 we can see that torque has much more oscillation than normal and in figure 3.27 which is related to speed it is obvious that speed doesn't follow the gear ratio.

3.4 Efficiency Computations and Comparison With Conventional Form

As mentioned before, in static analysis, one of rotors is steady and the other one is rotating with constant speed. Hence, torque diagrams are sinusoidal. In steady state analysis inner and outer rotor rotate with constant speeds which satisfy gear ratio. Thus, in simulation's result two constant torques which satisfy gear ratio with small ripples is observed. However, in transient analyses we assume one of rotors as input and the other one as output. Let's say that inner rotor in input and outer rotor is output so that input rotates with constant speed and for outer rotor a mechanical load is connected. Consequently, outer rotor rotates freely and outer rotor's speed and torque after some oscillations should reaches to a value which satisfies gear ratio.

Now in this section, efficiency analyses have been done which in these analyses we can also see that we have better results. For efficiency analyses we consider

hysteresis loss for rotor cores and eddy current for magnets. With this assumption, we apply steady state analysis on IPM type magnetic gear and conventional form of magnetic gear. As mentioned before, in steady state we have two constant torques which satisfy gear ratio. Nevertheless, when considering losses, torques are not following gear ratio and torque ratio drops. Furthermore, when rotation speed of rotors increases, torque ratio drops more, loss rate increases and efficiency decreases. Fig.3.28 is steady state analysis of proposed magnetic gear which inner rotor rotates with 330 min^{-1} and outer rotor rotates with 60 min^{-1}. It is obvious from this figure that torque ratio despite of speed ratio, is not according to gear ratio. Hence, efficiency is lower than 100 percent. According to Fig.3.28, inner rotor's torque is equal to 19.47 N.m and outer rotor torque is equal to 101.83 N.m .

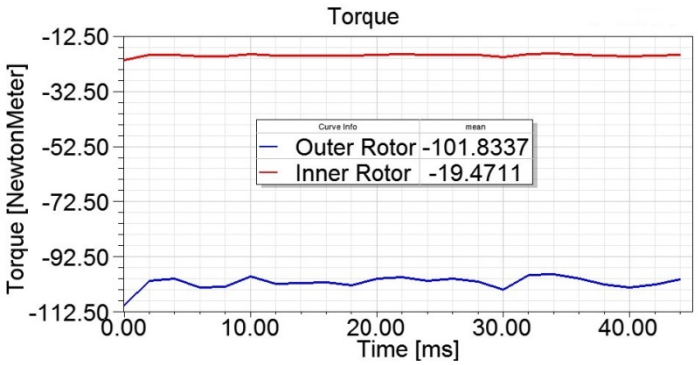

Figure 3.28: Steady state analysis of the proposed gear considering loss at speed of 60/330 min^{-1}.

$$P_{out} = w_{out}T_{out} = \frac{2\pi}{60} \times 60 \times 101.83 = 639.816\ W \qquad (\mathbf{3.4})$$

$$P_{in} = w_{in}T_{in} = \frac{2\pi}{60} \times 330 \times 19.47 = 672.835\ W \qquad (\mathbf{3.5})$$

$$\eta = \frac{P_{out}}{P_{in}} \times 100 = 95\% \qquad (\mathbf{3.6})$$

$$P_{loss} = P_{in} - P_{out} = 33.01\ W \qquad (\mathbf{3.7})$$

Figure 3.29 is result of the steady state analysis for the conventional form of gear considering loss.

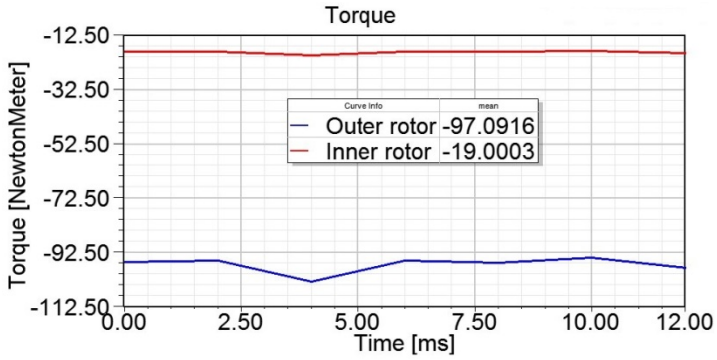

Figure 3.29: Steady state analysis of the conventional MG considering loss at speed of 60/330 min^{-1}.

$$P_{out} = w_{out}T_{out} = \frac{2\pi}{60} \times 60 \times 97.09 = 614.034\ W \qquad (\mathbf{3.8})$$

$$P_{in} = w_{in}T_{in} = \frac{2\pi}{60} \times 330 \times 19.00 = 656.593\ W \qquad (\mathbf{3.9})$$

$$\eta = \frac{P_{out}}{P_{in}} \times 100 = 93\% \qquad (\mathbf{3.10})$$

$$P_{loss} = P_{in} - P_{out} = 46.715\ W \qquad (\mathbf{3.11})$$

Consequently we can see that the efficiency in the proposed gear is better than the conventional form. For next step, rotation speed of rotors will be increased. It is assumed inner rotor's velocity 6600 min^{-1} and outer rotor's velocity 1200 min^{-1}. Thus, steady state analysis and the efficiency computation will be applied on the proposed magnetic gear and the conventional magnetic gear and then comparison will be presented. Figure 3.30 belongs to IPM type MG steady state analysis at 1200/6600 min^{-1} and Fig.3.31 belong to conventional MG under same conditions.

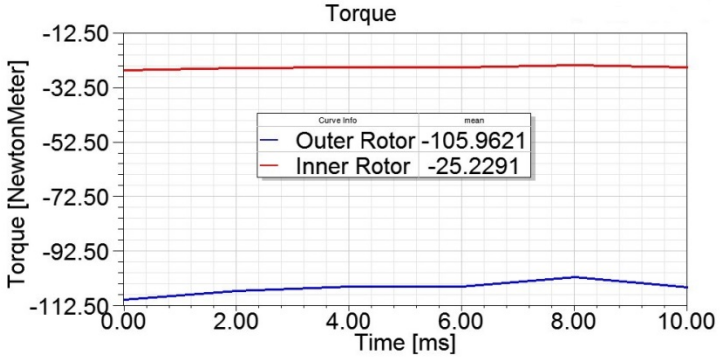

Figure 3.30: Steady state analysis of the proposed gear considering loss at 1200/6600 min^{-1}.

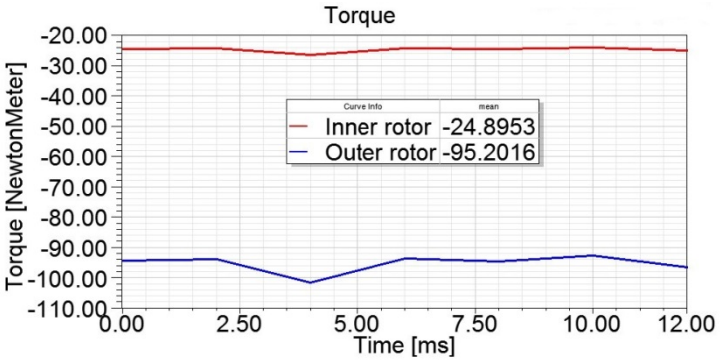

Figure 3.31: Steady state analysis of the conventional gear considering loss at 1200/6600 min^{-1}.

Using same equations which are mentioned before, we can compute efficiency of two magnetic gears. Following equations are related to proposed magnetic gear efficiency calculations:

$$P_{out} = w_{out}T_{out} = \frac{2\pi}{60} \times 1200 \times 105.96 = 13.315\ kW \qquad (\mathbf{3.12})$$

$$P_{in} = w_{in}T_{in} = \frac{2\pi}{60} \times 6600 \times 25.23 = 17.437\ kW \qquad (\mathbf{3.13})$$

$$\eta = \frac{P_{out}}{P_{in}} \times 100 = 76\% \qquad (\mathbf{3.14})$$

$$P_{loss} = P_{in} - P_{out} = 4.122\ kW \qquad (\mathbf{3.15})$$

And following equations are related to conventional magnetic gear efficiency calculations:

$$P_{out} = w_{out}T_{out} = \frac{2\pi}{60} \times 1200 \times 95.2 = 11.963\ kW \qquad (\mathbf{3.16})$$

$$P_{in} = w_{in}T_{in} = \frac{2\pi}{60} \times 6600 \times 24.4 = 16.864\ kW \qquad (\mathbf{3.17})$$

$$\eta = \frac{P_{out}}{P_{in}} \times 100 = 70\% \qquad (\mathbf{3.18})$$

$$P_{loss} = P_{in} - P_{out} = 4.901\ kW \qquad (\mathbf{3.19})$$

For the last analyses, inner and outer rotor speed will be increased. Inner rotor rotates with 13200 min^{-1} and outer rotor rotates with 2400 min^{-1}. Figure 3.32 is related to the steady state analysis considering loss for the proposed magnetic gear and Fig.3.33 is related to the conventional magnetic gear.

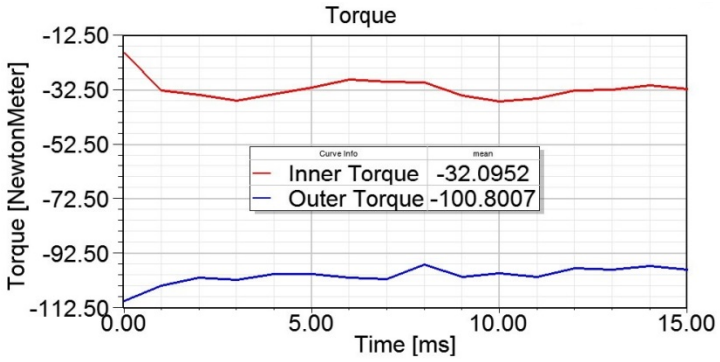

Figure 3.32: Steady state analysis of the proposed MG considering loss at 2400/13200 min^{-1}.

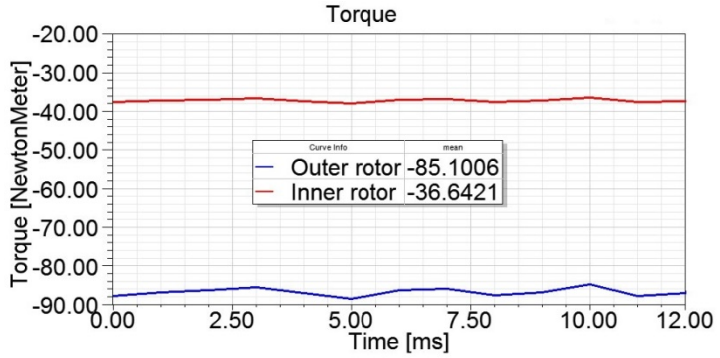

Figure 3.33: Steady state analysis of the conventional MG considering loss 2400/13200 min^{-1}.

Efficiency calculations for the proposed magnetic gear related to Fig.3.32:

$$P_{out} = w_{out}T_{out} = \frac{2\pi}{60} \times 2400 \times 100.8 = 25.33\ kW \quad (\mathbf{3.20})$$

$$P_{in} = w_{in}T_{in} = \frac{2\pi}{60} \times 13200 \times 32.1 = 44.371\ kW \quad (\mathbf{3.21})$$

$$\eta = \frac{P_{out}}{P_{in}} \times 100 = 57\% \quad (\mathbf{3.22})$$

$$P_{loss} = P_{in} - P_{out} = 19.038\ kW \quad (\mathbf{3.23})$$

Also for the conventional form:

$$P_{out} = w_{out}T_{out} = \frac{2\pi}{60} \times 2400 \times 85.1 = 21.387\ kW \quad (\mathbf{3.24})$$

$$P_{in} = w_{in}T_{in} = \frac{2\pi}{60} \times 13200 \times 36.64 = 50.647\ kW \quad (\mathbf{3.25})$$

$$\eta = \frac{P_{out}}{P_{in}} \times 100 = 42\% \quad (\mathbf{3.26})$$

$$P_{loss} = P_{in} - P_{out} = 29.26\ kW \quad (\mathbf{3.27})$$

Table 3.6: Efficiency and loss versus velocity of the conventional and the proposed magnetic gear.

Outer and inner rotor's speeds (min^{-1})	Output power of the proposed MG	Output power of the conventional MG	Efficiency of the proposed magnetic gear	Efficiency of the conventional magnetic gear	Loss of the proposed magnetic gear	Loss of the conventional magnetic gear
60/330	639.8 W	614 W	95%	93%	33 W	46.7 W
1200/6600	13.3 kW	11.9 kW	76%	70%	4.1 kW	4.9 kW
2400/13200	25 kW	21.38 kW	57%	42%	19 kW	29.3 kW

Consequently, increasing rotation speed will causes increasing the total loss, moreover, in structure which is introduced in this project, efficiency is higher than conventional for and loss rate is reduced. Table 3.6 shows the summary of this section.

4. CONCLUSION AND DISCUSSIONS

As a conclusion, according to Table 3.5, the proposed IPM type magnetic gear has better performance than other types of magnetic gear. Peak value of the proposed magnetic gear's static torque is quale to 310 N.m , however, in conventional magnetic gear the peak value of static torque is equal to 283 N.m . The goal for introducing this new structure was proposing a configuration which has higher performance while cost of constructing of the gear is constant or lower. According to the analyses which have been done in section 3.1 and presented in Table 3.2 and Table 3.3 using neodymium (NdFeB) is the best idea for using in magnetic gear because it is economical. Hence, if we want to use other type of magnet, due to generating same flux and obtaining same efficiency, we need to increase the cost. Consequently we decided to use neodymium as magnetic material. In section 3.2 we tested three various types of magnetic gear spoke type magnetic gear, surface mounted which are presented before and IPM type (proposed) magnetic gear which is new configuration. According to analyses that have been done among structures that are introduced before, surface mounted magnetic gear has better performance and higher torque capability. Moreover, the proposed gear has even higher performance that surface mounted magnetic gear. To prove this idea we have done static, steady state in section 3.2. Thus, according to analyses results the magnetic gear can handle more loads, because peak value of static torque is greater than surface mounted magnetic gear. In other words, torque has been increased nearly 10% in comparison with conventional form considering same dimensions. In section 3.3 some transient analyses and in section 3.4 efficiency computation and comparison with surface mounted magnetic gear have been applied. Also, in this section it has been proved that the proposed gear has lower rate of loss and higher rate of efficiency especially in higher speeds. For further works, it is assumed to increase gear ratio to 1:11. In the proposed magnetic gear, gear ratio is 1:5.5, however, due to implementing magnetic gear with a generator, increasing the gear ratio is needed. In next step, combination of magnetic gear and generator is considered (see Fig.4.1). Some papers have been published about this subject [72].

Nevertheless, the problem is that most of these structures have complexity. Furthermore, the goal is to improve their efficiency using new magnetic gear which has been proposed in this project.

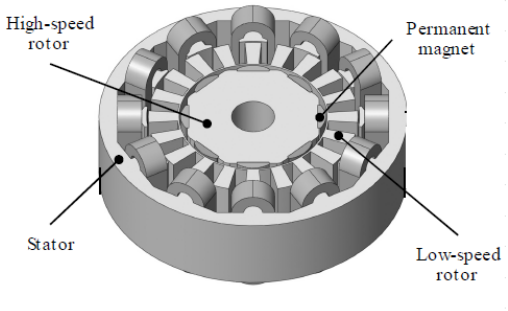

Figure 4.1: Combination of magnetic gear with generator [72].

REFERENCES

[1] **C.Armstrong** "power transmitting device" US patent 687 292, 1901.

[2] **A. Neuland,** "Apparatus for transmitting power," US Patent 117 1351, 1916.

[3] **T. V. Zweigbergk,** "Electric change speed gearing for automobiles," US Patent 1292 218, 1919.

[4] **H. Faus,** "Magnet gearing" US Patent 2243 555, 1941.

[5] **R. Lee, E. Brewer and N. Schaffel,** "Processing of Neodymium-Iron-Boron melt-spun ribbons to fully dense magnets," IEEE Transactions on Magnetics, vol. 21, no. 5, pp. 1958-1963, Sep. 1985.

[6] **K. Tsurumoto and S. Kikuchi,** "A new magnetic gear using permanent magnet," IEEE Tran. Magn., vol. 23, no. 5, pp. 3622-3624, Sept. 1987.

[7] **K. Tsurumoto**, "power transmitting of magnetic gear using common meshing and insensibility to center distance," IEEE Translation journal on magnetics in japan, vol. 3, no. 7, july 1988

[8] **K. Atallah and D. Howe,** "A novel high-performance magnetic gear," IEEE TRANSACTIONS ON MAGNETICS, vol. 37, no. 4, pp. 2844–2846, 2001.

[9] **F. J. P.O. Rasmussen, T.O. Anderson and O. Nielsen,** "Development of a high performance magnetic gear," in Conference Record of the 38th IAS Annual Meeting in Industry Applications, vol. 3, 2003.

[10] **J. Wang and K. Atallah,** "Modeling and control of „pseudo" direct-drive brushless permanent magnet machines," in *Proc. IEEE Int. Conf. IEMDC 2009*, Miami, FL, pp. 870-875.

[11] **L. Shah, A. Cruden, and B. W. Williams,** "A magnetic gear box for application with a contra-rotating tidal turbine," in *Proc. IEEE 7th Int. Conf. PEDS 2007*, Bangkok, Thailand, pp. 989-993.

[12] **L. Jian, K.T. Chau, Y. Gong, J.Z. Jiang, C. Yu, and W. Li,** "Comparison of coaxial magnetic gears with different topologies," *IEEE Trans. Magn.*, vol. 45, no. 10, pp. 4526-4529, Oct. 2009.

[13] **L. Yong, X. Jingwei, P. Kerong, and L. Yongping,** "Principle and simulation analysis of a novel structure magnetic gear," in *Proc. IEEE Int. Conf. ICEMS 2008*, Wuhan, China, pp. 3845-3849.

[14] **C.C. Huang, M.C. Tsai, D.G. Dorrell, and B.J. Lin,** "Development of a magnetic planetary gearbox," *IEEE Trans. Magn.*, vol. 44, no. 3, pp. 403-412, Mar. 2008.

[15] **F.T. Jorgensen, T.O. Andersen, and P.O. Rasmussen,** "The cycloid permanent magnetic gear," *IEEE Trans. Ind. Appl.*, vol. 44, no. 6, pp. 1659-1665, Nov./Dec. 2008.

[16] **J. Rens, R. Clark, S. Calverley, K. Atallah, and D. Howe,** "A novel magnetic harmonic gear," *IEEE Trans. Ind. Appl.*, vol. 46, no. 1, pp. 206-212, Jan./Feb. 2010.

[17] **Karl-Heinrick Grote, Erikk. Antonsson**, "Mechanical engineering," hand book of springer, volume 10.

[18] **Siavash Pakdelian, Nicolas W. Frank, Hamid A. Toliyat,** "Principles of the Trans-Rotary Magnetic Gear," IEEE transaction on magnetics, vol. 49, no. 2, February 2013.

[19] **Wenlong Li, K. T. Chau, and J. Z. Jiang,** " Application of linear magnetic gears for Pseudo-direct-drive oceanic wave energy harvesting" IEEE transactions on magnetics, vol.47, no.10, October 2011

[20] **H. Hurvitz,** "Magnetic gearing system," US Patent 2 548 373, 1951.

[21] **J. Cluwen,** "Magnetic circuits and devices," US Patent 2 722 617, 1955.

[22] **M. Baermann,** "Permanent magnet device for generating electrical energy," US Patent 3 273 001, 1966.

[23] **G. Reese,** "Magnetic gearing arrangement," US Patent 3 301 091, 1967.

[24] **S. Rand,** S. Rand, "Magnetic transmission system," US Patent 3 523 204, 1970.

[25] **N. Laing,** "Magnetic transmission," US Patent 345 650, 1972.

[26] **N. Laing,** "Centrifugal pump with magnetic drive," US Patent 3 762 839, 1973.

[27] **D. Hesmondhalgh and D. Tipping,** "A multielement magnetic gear," IEEE PROCEEDINGS, vol. 127, 1980.

[28] **S. C. K. Atallah and D. Howe,** "High-performance magnetic gears," Journal of Magnetism and Magnetic Materials, pp. 272–276, 2004.

[29] **K.Tsurumoto,** "Some consideration on the improvement of performance characteristics of magnetic gear," IEEE TRANSACTION JOURNAL ON MAGNETICS IN JAPAN, vol. 4, no. 9, SEPTEMBER 1989.

[30] **K.Tsurumoto,** "Some consideration on the improvement of performance characteristics of magnetic gear," IEEE TRANSACTION JOURNAL ON MAGNETICS IN JAPAN, vol. 4, no. 9, SEPTEMBER 1989.

[31] **K.Tsurumoto,** "Generating mechanism of magnetic force in meshing area of magnetic gear using permanent magnet," IEEE TRANSACTION JOURNAL ON MAGNETICS IN JAPAN, vol. 6, no. 6, JUNE 1991.

[32] **K.Tsurumoto,** "Basic analysis on transmitted force of magnetic gear using permanent magnet," IEEE TRANSACTION JOURNAL ON MAGNETICS IN JAPAN, vol. 7, no. 6, 1992.

[33] **N. T. K. Tsurumoto, S. Togo and S. Okano,** "Characteristics of the magnetic gear using a bulk hightc superconductor," IEEE TRANSACTIONS ON APPLIED SUPERCONDUCTIVITY, vol. 12, no. 1, MARCH 2002.

[34] **S. Kikuchi,** "Design and characteristics of a new magnetic worm gear using permanent magnet," IEEE TRANSACTIONS ON MAGNETICS, vol. 29, no. 6, NOVEMBER 1993.

[35] **S. Kikuchi and K. Tsurumoto,** "Trail construction of a new magnetic skew gear using permanent magnet," IEEE TRANSACTIONS ON MAGNETICS, vol. 30, no. 6, NOVEMBER 1994.

[36] **J.-P. H. Kyung-Ho Ha and Y.-J. Oh,** "Design and characteristic analysis of non-contact magnet gear for conveyor by using permanent magnet," in 37th IAS Annual Meeting in Industry Applications Conference, 2002.

[37] **C. H. D. C. S. W. Y.D. Yao, D.R. Haung and T. Ying,** "The radial magnetic coupling studies of perpendicular magnetic gears," IEEE TRANSACTIONS ON MAGNETICS, vol. 32, no. 5, 1996.

[38] **S. L. Y.D. Yao, D.R. Haung and S. Wang,** "Theoretical computations of the magnetic coupling between magnetic gears," IEEE TRANSACTIONS ON MAGNETICS, vol. 32, no. 3, MAY 1996.

[39] **C. L. S. W. D. C. Y.D. Yao, D.R. Huang and T. Ying,** "Magnetic coupling studies between radial magnetic gears," IEEE TRANSACTIONS ON MAGNETICS, vol. 33, no. 5, SEPTEMBER 1997.

[40] **Y.D. Yao, D.R. Huang and S. Wang,** "Simulation study of the magnetic coupling between radial magnetic gears," IEEE TRANSACTIONS ON MAGNETICS, vol. 33, no. 2, MARCH 1997.

[41] **E. Furlani,** "A two-dimensional analysis for the coupling of magnetic gears," IEEE TRANSACTIONS ON MAGNETICS, vol. 33, no. 3, MAY 1997.

[42] **J. W. K. Atallah and D. Howe,** "A high-performance linear magnetic gear," JOURNAL OF APPLIED PHYSICS 97, vol. 10N516, 2005.

[43] **S. C. J. Rens, K. Atallah and D. Howe,** "A novel magnetic harmonic gear," in IEEE International Electric Machines & Drives Conference IEMDC '07, 2007.

[44] **J. J. C. L. K.T. Chau, D. Zhang and Y. Zhang,** "Design of a magnetic-geared outer-rotor permanentmagnet brushless motor for electric vehicles," IEEE TRANSACTIONS ON MAGNETICS, vol. 43, pp. 2504–2506, 2007.

[45] **Y. Z. S. Du and J. Jiang,** "Research on a novel combined permanent magnet electrical machine," in International Conference of Electrical Machines and Systems, ICEMS, 2008.

[46] **K. C. L. Jian and J. Jiang,** "An integrated magnetic-geared permanent-magnet in-wheel motor for electric vehicles," in IEEE Vehicle Power and Propulsion Conference (VPPC), 2008.

[47] **K. C. L. Jian and J. Jiang,** "A magnetic-geared outer-rotor permanent-magnet brushless machine for wind power generation," IEEE TRANSACTIONS ON INDUSTRY APPLICATIONS, vol. 45, no. 3, pp. 954–962, MAY/JUNE 2009.

[48] **A. B. W. Hafla and W. Rucker,** "Efficient design analysis of a novel magnetic gear on a high performance computer," The International Journal for Computation and Mathematics in Electrical and Electronic Engineering, vol. 26, no. 3, pp. 712–726, 2007.

[49] **Y.W. L.L.Wang, J.X. Shen and K.Wang,** "A novel magnetic-geared outer-rotor permanent-magnet brushless motor," Power Electronics, Machines and Drives, PEMD, pp. 33–36, 2008.

[50] **P. L.W. F. C.W. L.L.Wang, J.X. Shen and H. Hao,** "Development of a magnetic-geared permanentmagnet brushless motor," IEEE TRANSACTIONS ON MAGNETICS, vol. 45, no. 10, pp. 4578–4581, OCTOBER 2009.

[51] **R. C. J. R. K. Atallah, S. Calverley and D. Howe,** "A new pm machine topology for low-speed, high-torque drives," in Proceedings of the 2008 International Conference on Electrical Machines, 2008.

[52] **S. M. K. Atallah, J. Rens and D. Howe,** "A novel "pseudo" direct-drive brushless permanent magnet machine," IEEE TRANSACTIONS ON MAGNETICS, vol. 55, no. 11, pp. 4349–4352, 2008.

[53] **A. Reinap and F. Marquez,** "Development of a modular linear magnetic gear as a project in the electrical engineering education," in Proceedings of the 2008 International Conference on Electrical Machines, 2008.

[54] **M.W. K. Davey and G.Wedeking,** "Magnetic gears - an essential enabler for the next generation's electromechanical drives," in ELECTRICAL MACHINES TECHNOLOGY SYMPOSIUM, (EMTS), 2008.

[55] **L. Jian and K. Chau,** "Analytical calculation of magnetic field distribution in coaxial magnetic gears," Progress in Electromagnetics Research, PIER 92, pp. 1–16, 2009.

[56] **L. Jian and K. Chau,** "Design and analysis of an integrated halbach-magnetic-geared permanentmagnet motor for electric vehicles," Journal of Asian Electric Vehicles, vol. 7, no. 1, pp. 1213–1219, 2009.

[57] **J. J. X. Liu, K.T. Chau and C. Yu,** "Design and analysis of interior-magnet outer-rotor concentric magnetic gears," JOURNAL OF APPLIED PHYSICS 105, vol. 07f101, 2009.

[58] **N. Frank and H. Toliyat,** "Gearing ratios of a magnetic gear for marine applications," in IEEE Electric Ship Technologies Symposium, ESTS., 2009.

[59] **N. Frank and H. Toliyat,** "Gearing ratios of a magnetic gear for wind turbines," in IEEE International Electrical Machines and Drives Conference, IEMDC'09., 2009.

[60] **H. T. H. M. P.O. Rasmussen, T.M. Jahns and T. Matzen,** "Motor integrated permanent magnet gear with a wide torque-speed range," in IEEE Energy Conversion Congress and Exposition, ECCE., 2009.

[61] **W. Fu and S. Ho,** "A quantitative comparative analysis of a novel flux-modulated permanentmagnet motor for low-speed drive," IEEE TRANSACTIONS ON MAGNETICS, vol. 46, pp. 127–134, 2010.

[62] **Vedanadam M. Acharya, Jonathan Z. Bird, and Matthew Calvin,** "A Flux Focusing Axial Magnetic Gear ," IEEE TRANSACTIONS ON MAGNETICS, VOL. 49, NO. 7, JULY 2013.

[63] **Krishna K. Uppalapati, Walter B. Bomela, Jonathan Z. Bird, Matthew D. Calvin,** "Experimental Evaluation of Low-Speed Flux-Focusing Magnetic Gearboxes" IEEE TRANSACTIONS ON INDUSTRY APPLICATIONS, VOL. 50, NO. 6, NOVEMBER/DECEMBER 2014.

[64] **Walter Bomela, Jonathan Z. Bird, and Vedanadam M. Acharya,** "The Performance of a Transverse Flux Magnetic Gear " IEEE TRANSACTIONS ON MAGNETICS, VOL. 50, NO. 1, JANUARY 2014.

[65] **Shan Peng, W. N. Fu, and S. L. Ho**, "A Novel Triple-Permanent-Magnet-Excited Hybrid-Flux Magnetic Gear and Its Design Method Using 3-D Finite Element Method" IEEE TRANSACTIONS ON MAGNETICS, VOL. 50, NO. 11, NOVEMBER 2014.

[66] **Mu Chen, K. T. Chau, Wenlong Li, and Chunhua Liu**, "Cost-Effectiveness Comparison of Coaxial Magnetic Gears With Different Magnet Materials" IEEE TRANSACTIONS ON MAGNETICS, VOL. 50, NO. 2, FEBRUARY 2014.

[67] **Yiduan Chen, Wei Nong Fu, Siu Lau Ho, and Huijuan Liu**, "A Quantitative Comparison Analysis of Radial-Flux, Transverse-Flux, and Axial-Flux Magnetic Gears" IEEE TRANSACTIONS ON MAGNETICS, VOL. 50, NO. 11, NOVEMBER 2014.

[68] **Thierry Lubin, Smail Mezani, and Abderrezak Rezzoug**, "Development of a 2-D Analytical Model for the Electromagnetic Computation of Axial-Field Magnetic Gears" IEEE TRANSACTIONS ON MAGNETICS, VOL. 49, NO. 11, NOVEMBER 2013.

[69] **A. Ragheb and M. Ragheb,** "Wind turbine gearbox technologies," in Proceedings of the 1st International Nuclear and Renewable Energy Conference (INREC10), 2010.

[70] **Wang, M.J. Kamper and J. Gieras,** "Optimal design of a coreless stator axial flux permanent-magnet generator," IEEE TRANSACTIONS ON MAGNETICS, vol. 41, pp. 55–64, 2005.

[71] **Marlin O.Thurston,** "Permanent Magnet Motor Technology" Electrical and computer engineering, a series of reference books and text books, second edition.

[72] **Noboru Niguchi and Katsuhiro Hirata**, "Torque-Speed Characteristics Analysis of a Magnetic-Geared Motor Using Finite Element Method Coupled With Vector Control", IEEE TRANSACTIONS ON MAGNETICS, VOL. 49, NO. 5, MAY 2013.

CURRICULUM VITAE

Name Surname: Sadra Mousavi

Place and Date of Birth: Urmia, Iran, 1989

E-Mail: sadramousavi@itu.edu.tr

EDUCATION: Studied B.Sc of electronics engineering at urmia university and currently student of Istanbul Technical University at master of electrical engineering.

B.Sc.: Urmia University (2012)